NATIONAL ADVISORY COMMITTEE FOR AERONAUTICS

TECHNICAL NOTE

No. 1683

AN EXPERIMENTAL INVESTIGATION OF AN NACA 63_1-012 AIRFOIL SECTION WITH LEADING-EDGE SUCTION SLOTS

By George B. McCullough and Donald E. Gault

Ames Aeronautical Laboratory,
Moffett Field, Calif.

Washington
August 1948

NATIONAL ADVISORY COMMITTEE FOR AERONAUTICS

TECHNICAL NOTE NO. 1683

AN EXPERIMENTAL INVESTIGATION OF AN NACA 63_1-012 AIRFOIL SECTION WITH LEADING-EDGE SUCTION SLOTS

By George B. McCullough and Donald E. Gault

SUMMARY

An NACA 63_1-012 airfoil section equipped with a single suction slot near the leading edge was investigated to determine whether or not the maximum lift coefficient could be increased by delaying the separation of flow at the leading edge characteristic of the basic section. The leading-edge separation was delayed and the linear portion of the lift curve substantially extended until the turbulent boundary layer separated from the rear portion of the airfoil. The abruptness of the stall was thereby reduced.

The maximum lift increased with increasing flow through the slot, rapidly at first, then at a diminishing rate. The effect on pitching moment was negligible. The profile drag was increased for low values of lift and reduced at high values of lift (for flow coefficients greater than 0.002) over the corresponding drag of the basic airfoil section.

It was found that the slot location and width are important. Sixteen different slots were investigated without encountering the optimum, but the results indicated that the leading edge of the slot should be downstream of the point of separation of flow from the leading edge of the basic airfoil immediately prior to its stall.

INTRODUCTION

The efficacy of boundary-layer control as a means of delaying separation of the turbulent boundary layer, and thereby increasing the lift of airplane wings, has been demonstrated by numerous small-scale experiments. Despite the favorable results of these experiments, few, if any, practical applications to conventional wings of moderate thickness have resulted because simpler high-lift devices were capable of producing adequate lift.

The trend toward thin swept wings for high-speed airplanes has made the attainment of sufficiently high maximum lift coefficients for landing more difficult. Airfoils suitable for high speed are generally characterized by undesirable stalling properties and relatively low maximum lift coefficients even when equipped with the most effective of flaps. For this reason, a research program was instituted to investigate the possibilities of increasing the maximum lift and improving the stalling properties of such airfoil sections by means of boundary-layer control.

Before attempting an application of boundary-layer control, the stalling and boundary-layer characteristics of two low-drag airfoil sections were investigated. It was found that the thicker of the two sections, an NACA 63_3-018, stalled because of separation of the turbulent boundary layer. The separated area originated at the trailing edge and spread progressively forward along the surface with increasing angle of attack. The thinner section, an NACA 63_1-012, stalled completely and abruptly because of separation of flow from the leading edge. These results made it obvious that, in order to increase the maximum lift of the thinner airfoil section, it would first be necessary to delay the leading-edge separation. If this could be done successfully, further increases in maximum lift probably could be achieved by controlling the turbulent boundary-layer over the aft portion of the airfoil (an application of boundary-layer control which has been successfully demonstrated in the past, e.g., references 1 and 2). In spite of its relatively large maximum section lift coefficient, the 12-percent-thick section was selected for use in the present investigation because of its abrupt stalling properties. Also the already existing boundary-layer data for this section would be of value for purposes of comparison with those of the suction airfoil.

This report presents the results of an experimental investigation to determine whether or not leading-edge separation can be forestalled by means of a single suction slot, and, to a lesser extent, to determine the optimum location and width of the slot. Only sharp-edged slots with their inlets approximately normal to the surface were considered. No attempt was made to find the optimum slot-entry shape.

Sixteen different slots near the nose of an NACA 63_1-012 airfoil were investigated separately. The data obtained include force, pressure, and boundary-layer measurements. The investigation was conducted in the Ames 7- by 10-foot wind tunnel No. 1.

SYMBOLS

The symbols used in this report are defined as follows:

c wing chord, 5.000 feet

c_{d_o} suction profile-drag coefficient (corrected for jet-boundary effect by the method of reference 3) $(D/q_o c)$

c_l section lift coefficient (corrected for jet-boundary effect by the method of reference 3) $(L/q_o c)$

c_m section pitching-moment coefficient referred to c/4 (corrected for jet-boundary effect by the method of reference 3) $(M/q_o c^2)$

c_q section flow coefficient $(Q/U_o c)$

D drag, pounds

H boundary-layer shape parameter (δ^*/θ)

L lift, pounds

M pitching moment, pound feet

p_l local static pressure, pounds per square foot

P_o free-stream static pressure, pounds per square foot

P pressure coefficient $\left(\frac{p_l - p_o}{q_o}\right)$

q_o free-stream dynamic pressure $(\frac{1}{2}\rho_o U_o^2)$, pounds per square foot

Q volume flow through slot per unit span at free-stream density, square feet per second

u local velocity inside boundary layer, feet per second

U local velocity outside boundary layer, feet per second

U_o free-stream velocity, feet per second

w slot width, feet

x distance from airfoil leading edge measured parallel to chord line, feet

x_u distance from airfoil leading edge to upstream edge of slot measured parallel to chord line, feet

y distance above airfoil measured normal to surface, feet

α_o section angle of attack (corrected for jet-boundary effect by the method of reference 1), degrees

δ total boundary-layer thickness, feet

δ_f flap deflection, degrees

δ^* boundary-layer-displacement thickness, feet

$$\left[\int_o^{\delta} \left(1 - \frac{u}{U}\right) dy \right]$$

θ boundary-layer-momentum thickness, feet

$$\left[\int_o^{\delta} \frac{u}{U} \left(1 - \frac{u}{U}\right) dy \right]$$

ρ_o free-stream mass density, slugs per cubic foot

MODEL AND APPARATUS

Model

The model used for this investigation was a 5-foot-chord, NACA 63_1-012, two-dimensional airfoil equipped with a 27-1/2-percent-chord plain flap hinged at the chord line. Circular end plates, 6 feet in diameter, attached to the model, formed part of the tunnel floor and ceiling. The model contained an internal plenum chamber to provide the ducting for the suction slot. The cross-section area of the plenum chamber was large enough to reduce the dynamic pressure of the induced air to negligible values, and to insure uniform flow into the slot across the 7-foot span of the model. Flush orifices in the surface of the model permitted measurement of the pressure distribution. Airfoil coordinates are given in table I, and a photograph of the model installed in the wind tunnel in figure 1.

The nose section of the model containing the slot was removable, facilitating changes in slot location and width. These dimensions varied from 0- to 1-percent chord in location, and from 0.167- to

0.800-percent chord in width (0.100- to 0.480 in.). Detailed dimensions of the 16 slots investigated are given in figure 2.

Apparatus

The suction required to induce flow into the slot was provided by a centrifugal blower outside the wind tunnel. The air duct to the blower left the lower end of the model through a mercury seal which isolated the model from mechanical forces introduced by the external piping.

The quantity of flow through the various slots was ascertained by measuring the pressure drop across an orifice meter built to American Society of Mechanical Engineers Standards. The air pressure within the plenum chamber was determined from three static-pressure tubes in the plenum chamber.

Boundary-layer velocity profiles were measured by means of a small rake or "mouse" attached to the surface of the airfoil. Several sizes of rakes were used, depending on the boundary-layer thickness. The smallest rakes (fig. 3) consisted of one static tube and six total-pressure tubes made of 0.015-inch-outside-diameter steel hypodermic tubing flattened to 0.007 inch at the ends. Larger rakes made of heavier tubing were capable of measuring boundary layers up to 4 inches in thickness.

In order to obtain indications of localized regions of separated flow over the surface, an adaptation of the liquid-film method was used. This technique, as originally developed in England for the purpose of ascertaining the point of transition from laminar to turbulent flow in the boundary layers of airfoils, depended on the difference in the rate of evaporation of a thin film of kerosene spread over the airfoil surface. For the adaptation employed in this investigation, a more volatile liquid was sprayed on the surface of the model. The boundary-layer flow scrubbed the liquid from the surface except under the region of separated flow where the lack of surface shear permitted the liquid to accumulate in a thick film. In order to make the liquid film more visible, the model was painted a dull black. The liquid was composed of 9 parts alcohol, 2 parts of 10-percent aqueous solution of Aerosol, and 1 part glycerin.

TESTS AND RESULTS

Method

The method of obtaining data was to maintain various constant values of the flow coefficient c_q as the angle of attack of the model was varied. Tests were made of each of the 16 slots at several values of the flow coefficient for the model with the flap undeflected, and at one value (c_q, 0.0025) with the flap deflected 40°. A full range of flow coefficients was employed, however, for the model with slot 15 and the flap deflected 40°.

Except for values of c_q greater than 0.005, all tests were made with a dynamic pressure of 40 pounds per square foot, which for the 5-foot-chord model corresponds to a Reynolds number of 5,800,000 and Mach number of 0.167. In order to obtain values of c_q greater than 0.005, it was necessary to reduce the dynamic pressure to 20 pounds per square foot, which corresponds to a Reynolds number of 4,150,000 and a Mach number of 0.116.

Lift, Moment, and Drag Measurements

Force measurements were made using the usual wind-tunnel balance system. The large number of these data makes a complete presentation impracticable, but typical lift and pitching-moment curves for the model with slot 15 are presented in figure 4. Force measurements of drag are not presented because of the unknown tare drag of the circular end plates attached to the model. Instead, the drag as evaluated from wake surveys is presented. Measurements made for the model with slot 15 are given in figure 5 as the variation of section profile drag coefficient with flow coefficient for constant values of lift. Also shown are the values of drag for the basic airfoil at the same values of lift.

A summary of the maximum lift obtained for the model, flap undeflected, with each of the 16 different slots is presented in figure 6. Each group of curves contains data for the model with slots of approximately the same width. The variations of maximum section lift coefficient with flow coefficient for the model with the flap deflected 40° and slot 15 are presented in figure 7.

Pressure-Distribution Measurements

Some typical pressure-distribution data obtained for the model with slot 15 are presented in figures 8 and 9. Also shown on these

plots are pressure distributions for the basic airfoil at maximum lift. The values of the pressure coefficient P are observed values at the test Mach number of 0.167 and have not been corrected to zero Mach number. Some of the values of the pressure coefficient observed upstream of the slot are greater than the maximum ordinate of the plots. To depict more clearly the pressure distribution in the immediate vicinity of the slot, the first 10 percent of the chord is shown to enlarged scale in figure 10. The scale of P has been compressed to keep the negative pressure peaks within the ordinate scale of the plots.

Some additional pressure distributions over the upper surface of the model are given in table II. These data are for the model with slot 15; flap undeflected and deflected 40°; c_q, 0.0038 and 0.0035, respectively. The angles of attack selected correspond to lift coefficients in the vicinity of the peaks of the lift curves.

Flow Visualization Studies

A limited investigation was made using the liquid-film method for the purpose of ascertaining the location and extent of the laminar separated region near the nose of the airfoil. The technique employed was to spray the model with a light coating of the liquid described under Apparatus, then to run the wind tunnel a short time with the model at a fixed angle of attack. At 8° angle of attack, a narrow spanwise band of liquid bounded by relatively dry areas was discernible on the basic airfoil. At higher angles of attack, the band became covered with a whitish, fine-grained froth which persisted on the airfoil after the tunnel was stopped. Measurements of the well-defined boundaries of the band are presented in figure 11. The band was taken to indicate a region in which the boundary-layer flow separated from the airfoil for a short distance along the surface, then reattached leaving beneath it a bubble of relatively dead air. This phenomenon was observed near the leading edge of the basic airfoil prior to the complete separation of flow. The visualization technique was applied to one slotted-airfoil configuration (slot 15) for flow rates greater than $c_q = 0.0012$, and for this case the phenomenon was not discernible.

Boundary-Layer Measurements

The results of boundary-layer surveys are shown in figures 12 and 13. These data were obtained for the model with slot 15, and are presented as the chordwise variations of the derived boundary-layer parameters, momentum thickness θ, and shape parameter H. In figure 12, the variations of the parameters are shown for two values of the section flow coefficient, and in figure 13 comparison

is made with the same boundary-layer characteristics of the basic airfoil

Plenum-Chamber Pressures

An indication of the pressure against which the boundary-layer suction pump must operate is given in figure 14. These data were obtained with slot 15 from the average readings of the three static tubes in the plenum chamber. The pressures are expressed in coefficient form in the same manner as the pressure over the surface of the airfoil.

No attempt was made to design an efficient expansion from the slot entry into the plenum chamber. Undoubtedly, the suction pressure could be reduced by careful design.

DISCUSSION

The Effect of Boundary-Layer Suction

Maximum lift. - Inspection of the summary plots of figures 6 and 7 shows that with no flow, all of the slots investigated reduced the maximum lift below that of the basic airfoil. The reductions in lift (and changes in the peak of the lift curve) are similar to the effects of standard roughness as discussed in reference 4. In general, the maximum lift increased rapidly with increasing flow coefficient up to a value of c_q of about 0.0025. Above this value, the maximum lift tended to increase more slowly and appeared to be approaching an ultimate value asymptotically. The two slots on the chord line (slots 1 and 2) were ineffective in increasing the maximum lift above that of the basic airfoil throughout the range of flow coefficients investigated.

To give an idea of the magnitude of the air flow into the slot, consider an airfoil of 10-foot chord at an airspeed of 100 miles per hour at sea level. A value of c_q of 0.0025 would correspond to a volume flow into the slot of about 3.7 cubic feet per second (at free-stream density) per foot of span or a weight rate of flow of about 0.28 pound per second per foot of span.

The greatest increment of lift was obtained with slot 15 which increased the $c_{l_{max}}$ from 1.38 for the basic airfoil to 1.84 at a value of c_q of 0.0068. Because of this fact, most of the data were obtained for the model with slot 15 which was the widest and farthest aft of the 16 slots investigated.

The effect of flow into the slot was to extend the straight portion of the c_l versus α curve to higher angles of attack, and

to round over the peak of the curve (fig. 4). There was no effect on the angle of attack for zero lift.

The stall of the basic airfoil was sharp and abrupt, shaking the model support system so violently that it was impossible to obtain satisfactory test points beyond the stall. This type of stall is considered dangerous in that the pilot of an airplane would have no warning of the imminence of the stall in the form of shaking or buffeting of the aircraft. With suction, the model stalled more gently, making it possible to obtain test points beyond the peak of the lift curve. This is considered indicative that the initial phase of the stall, at least, resulted from separation of the turbulent boundary layer at the trailing edge which would give warning to the pilot. This type of stall was similar to that characteristic of the basic section when equipped with a 10-percent-chord nose flap for the preliminary investigation.

Similar effects were observed with the flap deflected 40°. The maximum section lift coefficient was increased from 2.03 for the basic airfoil to 2.54 at a value of c_q of 0.0065.

Pitching moment.- The effect of boundary-layer suction on the pitching moment of the model both with the flap undeflected and deflected 40° was negligible. The pitching-moment curves (fig. 4) practically coincide throughout the linear range of lift coefficients.

Profile drag.- The profile drag of the airfoil, as measured by the wake survey method (fig. 5), decreased with increasing flow coefficient, rapidly at first, then at a diminishing rate. The drag of the airfoil with no flow into the suction slot was considerably larger than that of the basic airfoil for all values of lift, but, for a c_l of 0.8 and flow coefficients greater than about 0.002, the drag was slightly less than that of the basic airfoil. It should be mentioned that the measured values of drag do not include the sink drag of the air induced into the airfoil (i.e., the component of momentum of the induced air in the drag direction), nor is any consideration given to the power required to induce flow into the slot.

The pressure against which the boundary-layer suction pump must operate is high near maximum lift, as may be seen in figure 14. If the pumping power is charged against the aircraft power plant as drag, then the total wing drag will be high, but if excess power from the engine is available as in a normal landing approach, then the power required for boundary-layer control is of no consequence.

A calculation of the power required for boundary-layer control was made for the hypothetical 10-foot-chord airfoil mentioned in the discussion of lift. Assuming 100-percent-efficient air induction and using the values ($c_q = 0.0025$ and $P = -16$) corresponding to a

c_l of 2.2 with the flap down, the power required for the air pump is about 3 horsepower per foot of span at 100 miles per hour at sea level.

Pressure distribution.– The pressure distributions (fig. 10) show that with flow into the slot, the localized peak suction pressures were always greater than those on the basic airfoil at the same angle of attack, but the maximum suction pressure immediately downstream of the slot was always less than the local peak suction pressure in the immediate vicinity of the leading edge of the basic airfoil. The pressure distribution downstream of the 1-percent-chord station is nearly identical for the model with and without the slot.

Boundary-layer characteristics.– The decrease of boundary-layer thickness with increased flow through the slot may be seen in figure 12. The effectiveness of boundary-layer control in delaying complete separation of flow from the leading edge is indicated by the increased lift and stalling angle of the airfoil. The attainment by the shape parameter H of a value of 2.6 at the trailing edge is indicative that turbulent separation had occurred at this point. (Previous investigations have demonstrated that complete separation of the turbulent boundary layer starts when H attains a value of 2.6 to 2.7 (references 5 and 6).) Further verification that the turbulent boundary layer separated near the trailing edge with flow through the slot was given by tuft studies. It could not be demonstrated, however, that the complete stall was the result of the forward progression of the turbulent separated area. It is possible that separation from the leading edge may have spread rapidly downstream to merge with the turbulent separation spreading forward immediately prior to the complete stall of the airfoil.

At 0° angle of attack and with flow into the slot, the momentum thickness of the boundary layer was nearly twice that for the basic airfoil (fig. 13). At 4.2° angle of attack, the boundary layer of the suction airfoil was slightly thicker, and, at higher angles of attack, the boundary layer was appreciably thinner than that of the basic airfoil. The value of the shape parameter was slightly lower with boundary-layer control, particularly at the higher angles of attack, indicating a more stable turbulent boundary layer.

Since the pressure distribution over the suction airfoil and that over the basic airfoil were practically identical downstream of the station of the slot, differences in the rate of boundary-layer growth are not attributable to differences in the pressure gradient against which the boundary layer must flow. The observed velocity profiles showed that the effect of the slot was to cause earlier transition to turbulence at low angles of attack than was the case for the basic airfoil. Because of its more forward starting point,

the turbulent boundary layer thickened more rapidly than the boundary layer of the basic airfoil. At high angles of attack the initial thickness of the turbulent boundary layer was reduced because of the removal of the localized region of separated flow by the action of the slot. The effect of the suction slot may be seen in figure 15, in which are compared boundary-layer velocity profiles measured at the 10-percent-chord station on the basic and the suction airfoil. The turbulent boundary layer of the suction airfoil grew less rapidly because of its initial thinness. The slower rate of growth of an initially thin boundary layer may be seen in figure 13.

These effects of the suction slot on boundary-layer growth explain the drag results shown in figure 5.

The effectiveness of leading-edge suction in increasing the maximum lift coefficient of airfoils subject to leading-edge separation is the result of two effects of the suction slot. First, the leading-edge separation is prevented until the airfoil stalls at higher values of the lift coefficient. It has been shown that, for the same value of lift coefficient below the stall of the basic airfoil, the pressure distributions downstream of the station of the slot (figs. 8 and 9), and the boundary-layer characteristics (fig. 13) of the basic and suction airfoils are similar. The principle effect of the suction slot, therefore, is to delay separation of flow from the leading edge. Second, a further increase of maximum lift is achieved because at high values of lift the initial thickness of the turbulent boundary layer is reduced, enabling the turbulent boundary layer to make a greater pressure recovery before separating from the surface of the airfoil.

The Optimum Slot

It was believed that the important variables to be considered in selecting the optimum slot for increasing maximum lift were (1) the chordwise location of the upstream edge of the slot, and (2) the width of the slot. Accordingly, the maximum-lift data were cross-plotted in two different ways.

In figure 16, the maximum section lift coefficient is shown as a function of the chordwise location of the upstream edge of the slot. Data for four different widths of the slot are presented. The wider slots did not extend sufficiently far aft to define definitely the optimum location. For the narrowest slot (0.2 percent chord), the optimum location is about 0.5 percent chord. It is interesting to note that the downstream boundary of the froth band obtained in the liquid-film studies was also at 0.5 percent chord of the basic

airfoil immediately prior to the stall. (See fig. 11.) As the slot was widened, there appeared a tendency for the optimum location to move aft.

In figure 17, the maximum section lift coefficient is plotted against slot width for three different values of the flow coefficient. In general, it appears that within the range of slot widths investigated, the wider the slot the greater its effectiveness, particularly for the higher values of flow coefficient.

For the model with the flap deflected 40°, the same general trends are evident as for the model with the flap undeflected.

These data are insufficient for an exact determination of the optimum slot. Although greater values of lift may be obtained by use of a slot somewhat farther aft and wider than slot 15, it does not seem probable that the increase will be very large, as shown by the tendency of the curves of maximum lift coefficient to level off with increasing slot width.

CONCLUDING REMARKS

The leading-edge type of separation of flow which normally characterizes the stall of the NACA 63_1-012 airfoil section was successfully forestalled by means of a single suction slot near the nose of the airfoil. The maximum lift of the airfoil was thereby increased until the turbulent boundary layer separated from the trailing edge. Although it was not demonstrated that the complete stall was the result of turbulent separation, the abruptness of the stall was considerably alleviated from that of the basic airfoil section.

The largest increment of the maximum section lift coefficient realized was 0.46 with the flap undeflected and 0.51 with the plain flap deflected 40°. It is believed that somewhat greater increments of lift could be obtained with a slot of more nearly optimum width and location.

The chordwise location and width of the slot are important. The results of this investigation indicate that the leading edge of the slot should be downstream of the point of separation immediately prior to the stall of the basic section. The effectiveness of the slot increases with slot width up to a value of at least 0.8 percent chord.

Ames Aeronautical Laboratory,
National Advisory Committee for Aeronautics,
Moffett Field, Calif.

REFERENCES

1. Bamber, Millard J.: Wind Tunnel Tests on Airfoil Boundary Layer Control Using a Backward-Opening Slot. NACA Rep. No. 385, 1931.

2. Quinn, John H., Jr.: Wind-Tunnel Investigation of the NACA 65_4-421 Airfoil Section with a Double Slotted Flap and Boundary-Layer Control by Suction. NACA TN No. 1395, 1947.

3. Allen, H. Julian, and Vincenti, Walter G.: Wall Interference in a Two-Dimensional-Flow Wind Tunnel with Consideration of the Effect of Compressibility. NACA ARR No. 4K03, 1944.

4. Abbott, Ira H., von Doenhoff, Albert E., and Stivers, Louis S., Jr.: Summary of Airfoil Data. NACA ACR No. L5C05, 1945.

5. von Doenhoff, Albert E., and Tetervin, Neal: Determination of General Relations for the Behavior of Turbulent Boundary Layers. NACA Rep. No. 772, 1943.

6. Dryden, Hugh L.: Some Recent Contributions to the Study of Transition and Turbulent Boundary Layers. NACA TN No. 1168, 1947.

TABLE I.- COORDINATES FOR NACA 63_1-012 AIRFOIL SECTION

Station (percent chord)	Ordinate (percent chord)
0	0
.5	1.404
.75	1.713
1.25	2.717
2.5	3.104
5	4.362
7.5	5.308
10	6.068
15	7.225
20	8.048
25	8.600
30	8.913
35	9.000
40	8.845
45	8.482
50	7.942
55	7.256
60	6.455
65	5.567
70	4.622
75	3.650
80	2.691
85	1.787
90	.985
95	.348
100	0
Leading-edge radius 1.087-percent chord	

TABLE II.- MEASURED PRESSURE COEFFICIENTS P OVER THE UPPER SURFACE OF THE SUCTION AIRFOIL WITH SLOT 15

	$\delta_f = 0^o$; $c_q = 0.0038$							$\delta_f = 40^o$; $c_q = 0.0035$					
$\frac{x}{c}$ \ α_o	8.4	10.5	12.6	14.8	16.8	17.9	18.9	8.7	10.8	12.8	13.9	14.9	15.9
0	-3.780	-6.660	-9.510	-12.680	-15.380	-17.340	-17.860	12.810	-16.620	- - - -	- - - -	- - - -	- - - -
.0010	-6.630	-9.480	-13.580	-17.290	-23.350	- - - -	-26.100	-17.39	-23.380	-28.070	-28.620	-31.420	-30.820
.0033	-6.520	-8.810	-12.060	-14.920	-17.700	-19.360	-18.830	-15.140	-18.960	-19.690	-23.020	-25.500	-25.100
.0105	-3.368	-4.635	-6.260	-7.490	-8.270	-9.130	-9.195	-8.000	-9.360	-10.720	-10.800	-11.120	-11.110
.0125	-2.791	-3.870	-5.120	-6.275	-7.540	-7.950	-8.375	-6.759	-7.860	-8.970	-9.420	-9.743	-9.800
.0175	-2.867	-3.846	-4.990	-6.060	-7.310	-7.720	-8.050	-6.545	-7.560	-8.590	-8.990	-9.380	-9.380
.0250	-2.550	-3.354	-4.278	-5.125	-5.855	- - - -	- - - -	-5.570	-6.339	- - - -	- - - -	- - - -	- - - -
.0375	-2.120	-2.740	-3.439	-4.078	-4.705	-5.085	-5.215	-4.469	-5.070	-5.695	-5.918	-6.220	-6.100
.0500	-1.985	-2.520	-3.122	-3.663	-4.200	-4.523	-4.620	-4.050	-4.560	-5.080	-5.268	-5.530	-5.407
.0750	-1.702	-2.115	-2.573	-2.972	-3.380	-3.618	-3.688	-3.352	-3.730	-4.118	-4.250	-4.440	-4.335
.1000	-1.515	-1.850	-2.233	-2.545	-2.862	-3.070	-3.092	-2.930	-3.234	-3.532	-3.638	-3.800	-3.683
.1500	-1.266	-1.520	-1.794	-2.018	-2.255	-2.390	-2.409	-2.409	-2.620	-5.828	-2.904	-3.006	-2.904
.2000	-1.139	-1.340	-1.569	-1.740	-1.918	-2.030	-2.029	-2.152	-2.320	-2.471	-2.518	-2.600	-2.484
.2500	-1.054	-1.230	-1.410	-1.553	-1.698	-1.777	-1.774	-1.990	-2.120	-2.229	-2.260	-2.322	-2.204
.3000	-.975	-1.120	-1.280	-1.392	-1.506	-1.580	-1.559	-1.851	-1.950	-2.030	-2.054	-2.098	-1.973
.3500	-.900	-1.030	-1.155	-1.249	-1.347	-1.389	-1.380	-1.745	-1.810	-1.874	-1.884	-1.906	-1.779
.4000	-.816	-.925	-1.030	-1.095	-1.176	-1.206	-1.195	-1.612	-1.660	-1.700	-1.704	-1.704	-1.573
.4500	-.717	-.810	-.890	-.945	-1.000	-1.020	-1.000	-1.475	-1.500	-1.528	-1.511	-1.510	-1.363
.5000	-.618	-.700	-.770	-.801	-.835	-.854	-.835	-1.346	-1.355	-1.365	-1.341	-1.317	-1.174
.5500	-.524	-.584	-.640	-.622	-.684	-.692	-.686	-1.214	-1.210	-1.203	-1.175	-1.151	-1.010
.6000	-.431	-.475	-.515	-.527	-.538	-.542	-.530	-1.091	-1.070	-1.050	-1.020	-.984	-.852
.6500	-.337	-.375	-.400	-.408	-.407	-.409	-.410	-.990	-.950	-.908	-.869	-.844	-.752
.7000	-.248	-.281	-.300	-.298	-.291	-.283	-.300	-.908	-.860	-.792	-.738	-.714	-.684
.7500	-.154	-.166	-.190	-.189	-.201	-.202	-.235	-.673	-.634	-.599	-.568	-.572	-.642
.8000	-.099	-.106	-.120	-.129	-.141	-.141	-.190	-.673	-.634	-.599	-.572	-.578	-.642
.8500	-.020	-.030	-.045	-.050	-.080	-.090	-.195	-.683	-.644	-.609	-.578	-.588	-.652
.9000	.040	.040	.020	0	-.035	-.051	-.110	-.688	-.650	-.609	-.578	-.594	-.663
.9500	.099	.095	.080	.055	.010	-.015	-.065	-.684	-.640	-.604	-.572	-.598	-.668

Note: Upper surface is discontinuous between x/c = 0.00377 and x/c = 0.0100.

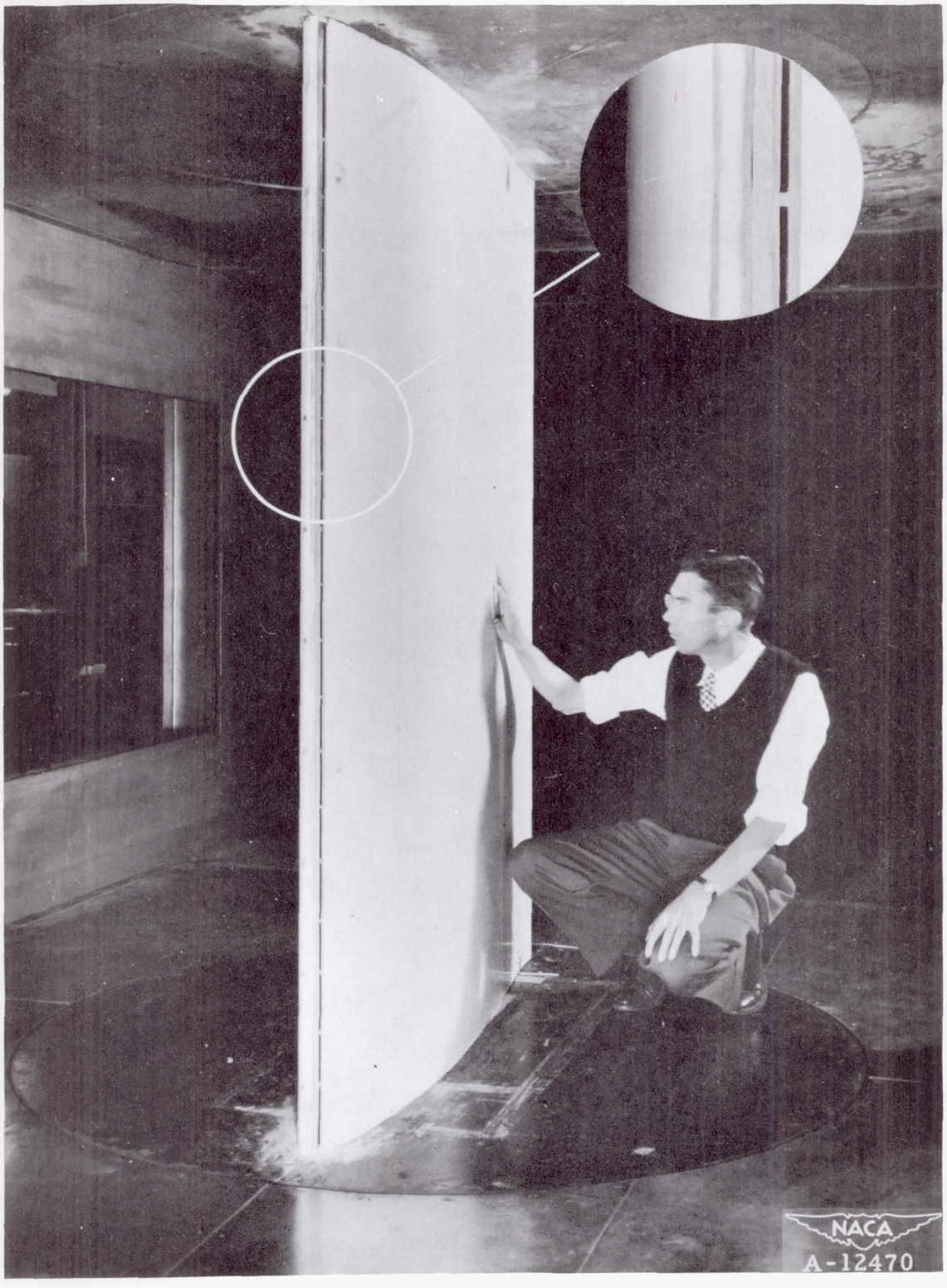

Figure 1.– Photograph of the NACA 63_1-012 airfoil model with nose-suction slot.

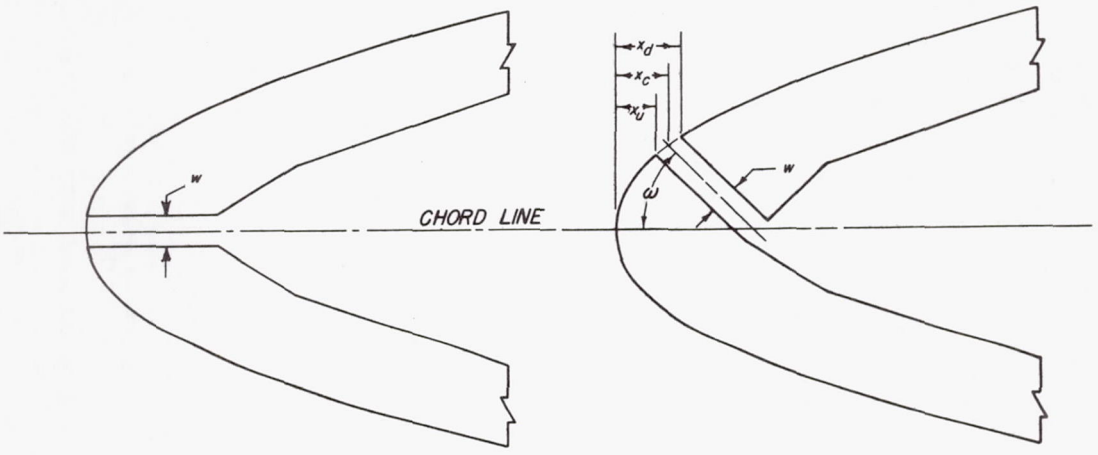

Slots 1–2 Slots 3 – 16

NOTE:-ALL DIMENSIONS ARE PERCENT OF THE WING CHORD

Slot No.	x_u	x_c	x_d	w	ω
1				0.167	
2				0.750	
3	0.267	0.317	0.367	0.167	45°
4	0.267	0.367	0.483	0.333	45°
5	0.267	0.425	0.600	0.500	45°
6	0.377	0.450	0.516	0.200	45°
7	0.516	0.590	0.667	0.200	45°
8	0.667	0.750	0.830	0.200	45°
9	0.830	0.917	1.000	0.200	45°
10	0.377	0.516	0.667	0.400	45°
11	0.516	0.667	0.830	0.400	45°
12	0.667	0.750	1.000	0.400	45°
13	0.377	0.590	0.830	0.600	45°
14	0.516	0.750	1.000	0.600	45°
15	0.377	0.667	1.000	0.800	45°
16	0.267	0.483	0.720	0.667	45°

Figure 2.- Geometry of the various slots investigated.

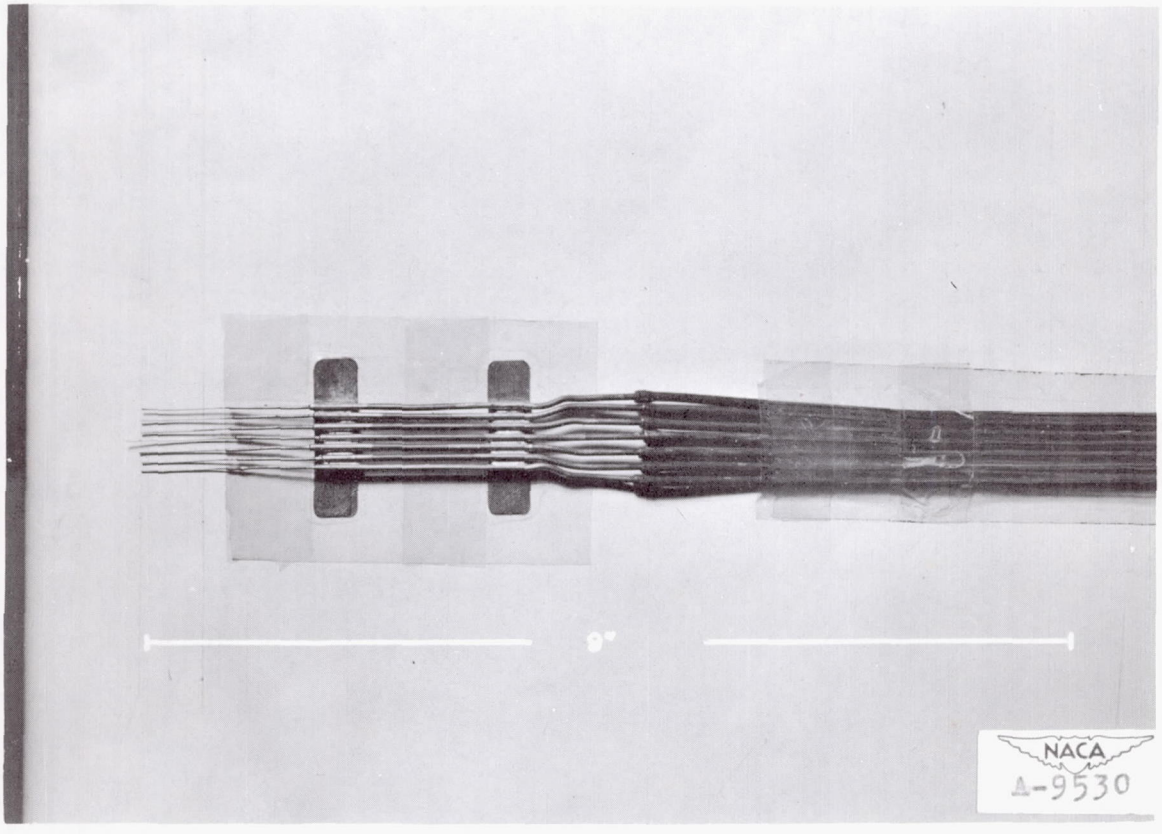

Figure 3.- Detail of small boundary-layer rake or "mouse."

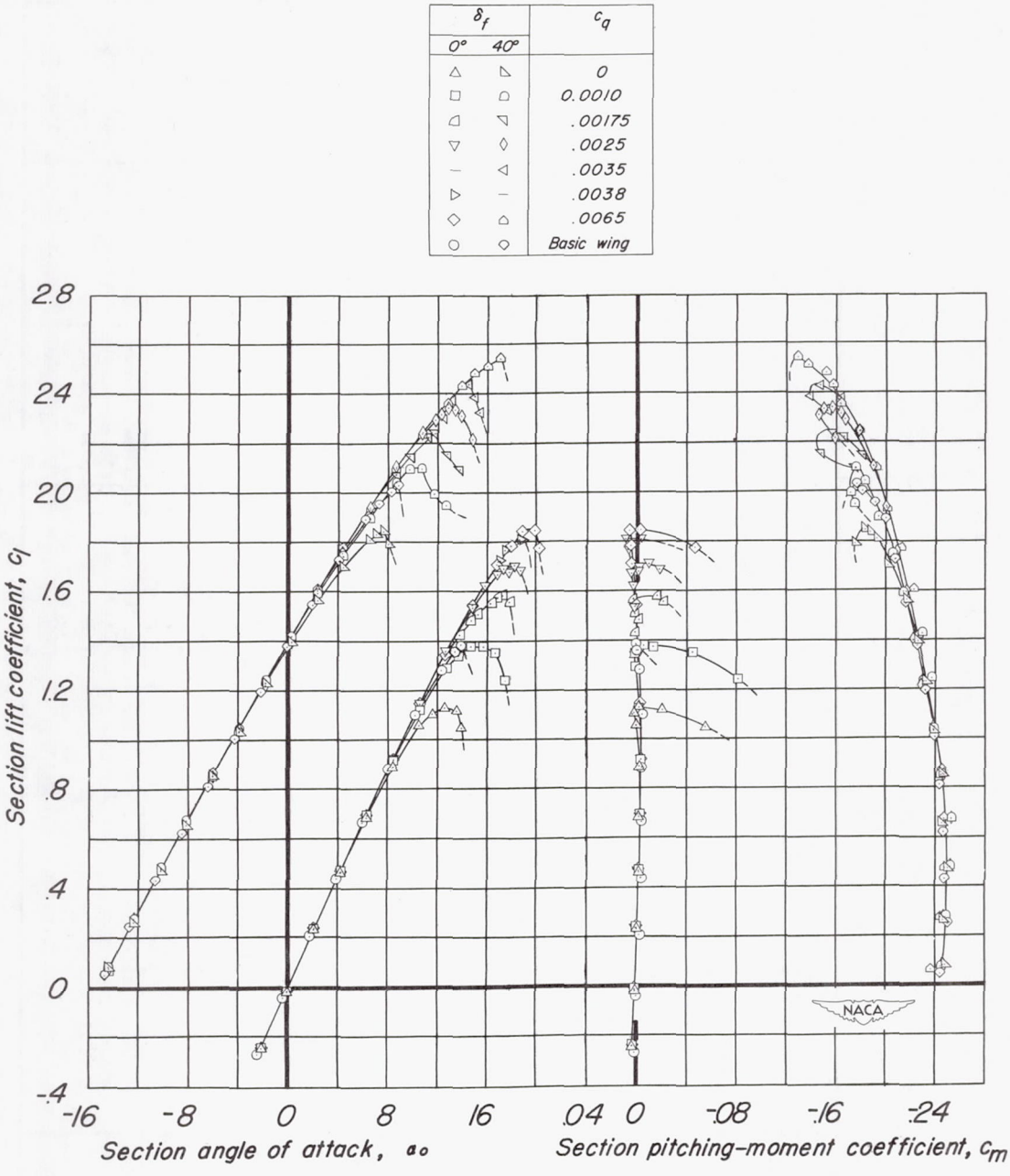

Figure 4.- Lift and pitching-moment characteristics of the model with slot 15.

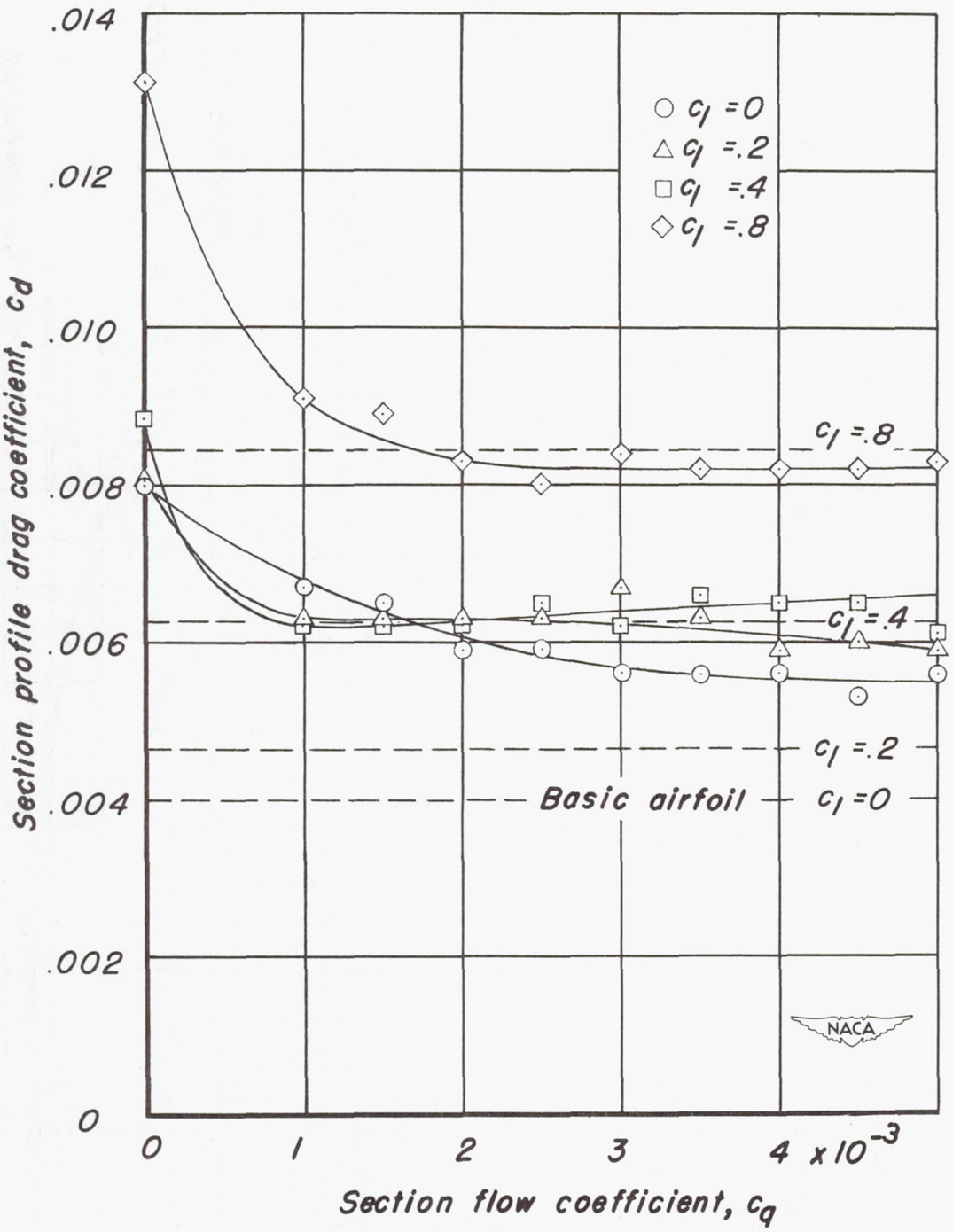

Figure 5. Variation of profile drag with flow coefficient for the model with slot 15.

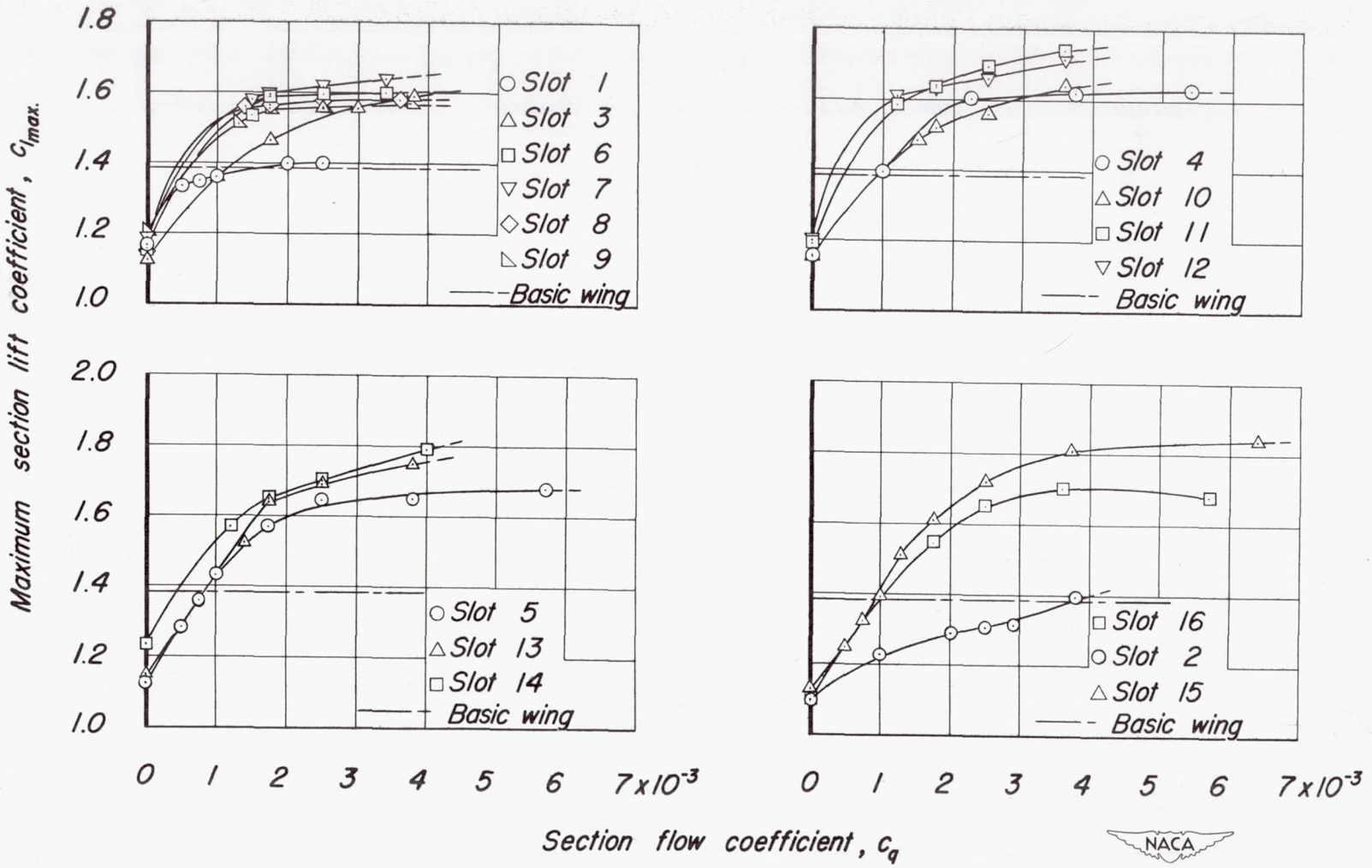

Figure 6.- Variation of maximum lift with flow coefficient for the model with flap undeflected.

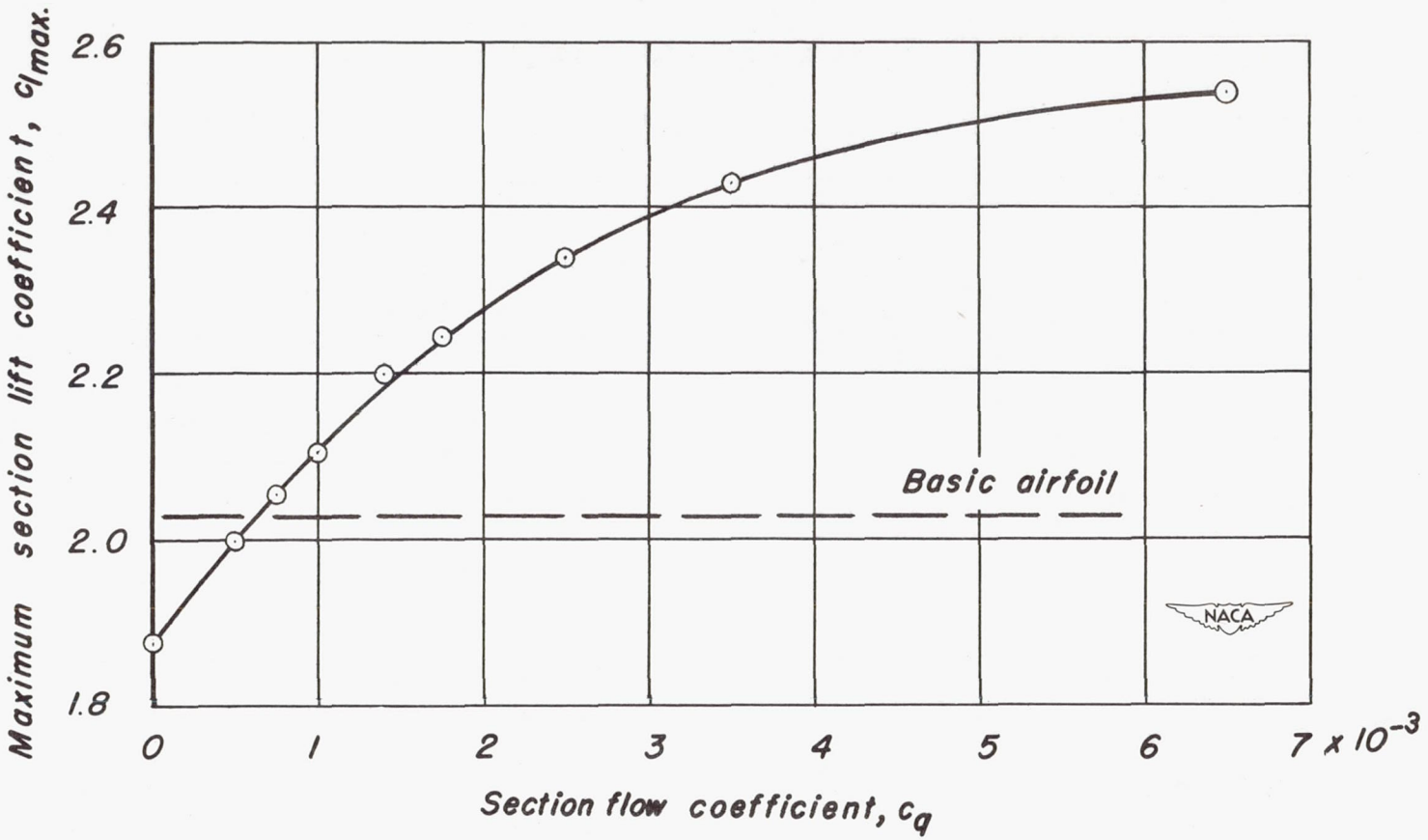

Figure 7.- Variation of maximum lift with flow coefficient for the model with the flap deflected 40°. Slot 15.

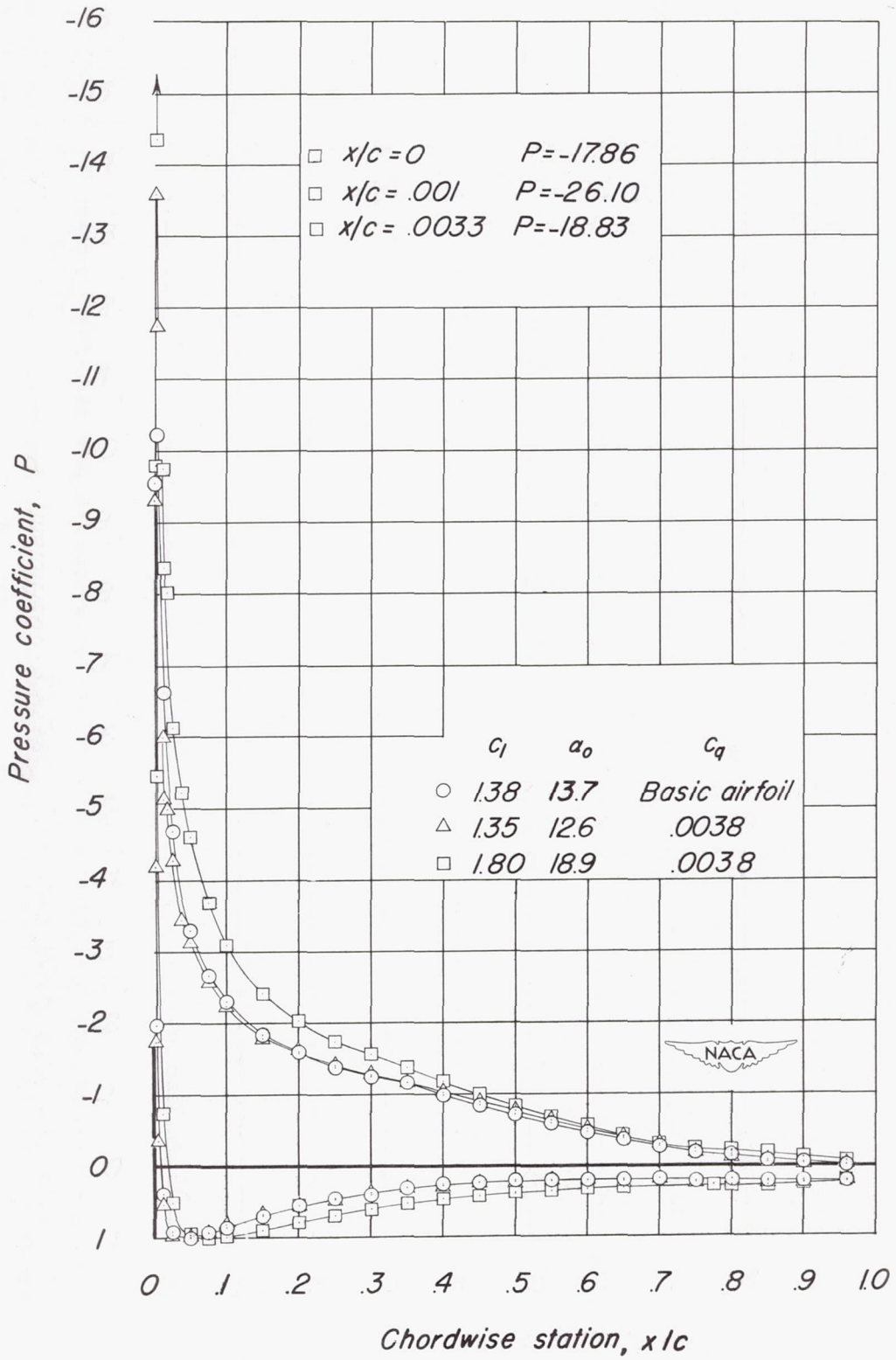

Figure 8.- Pressure distribution for the model with the flap undeflected. Slot 15.

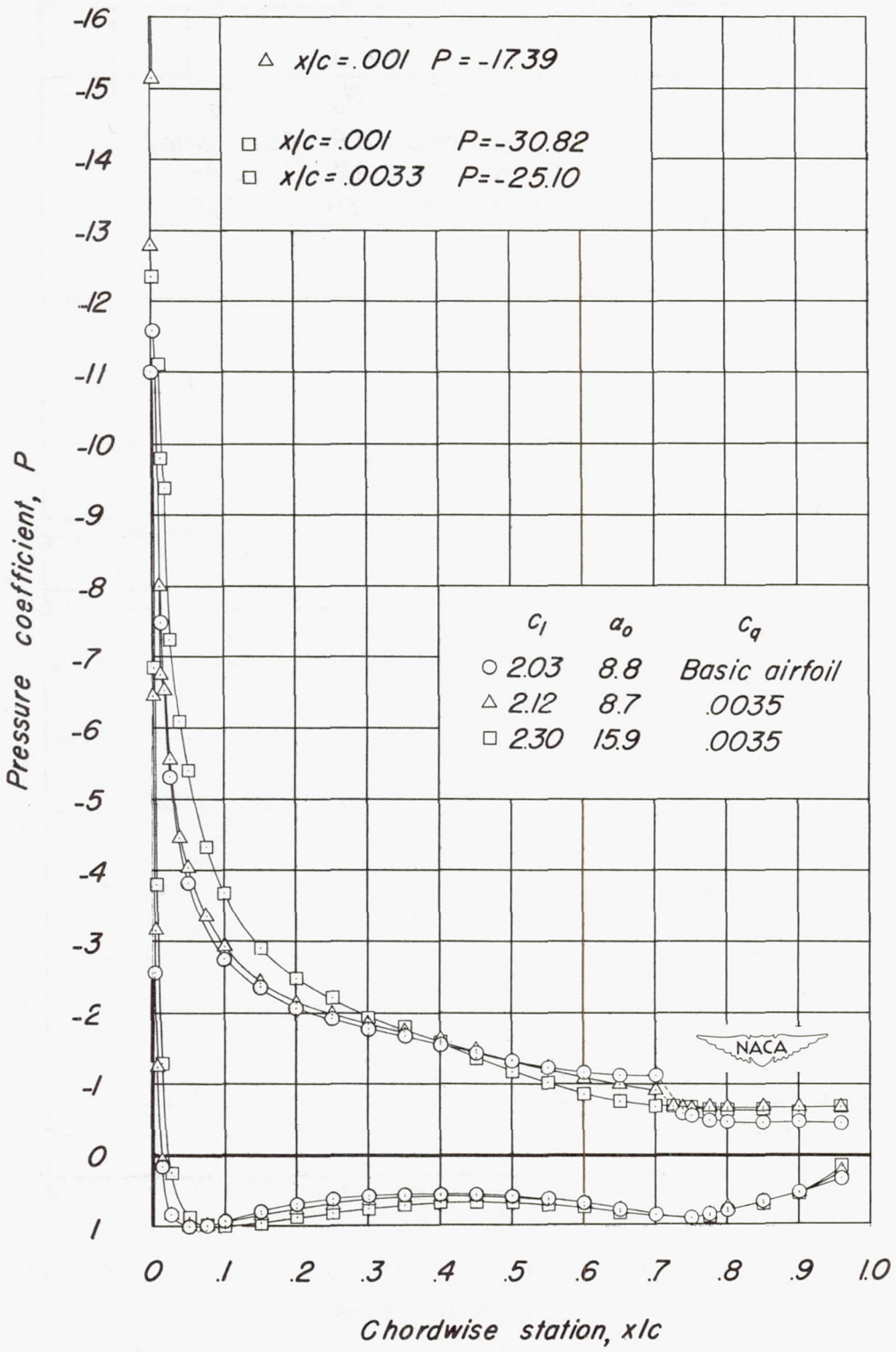

Figure 9.- Pressure distribution for the model with the flap deflected 40°. Slot 15.

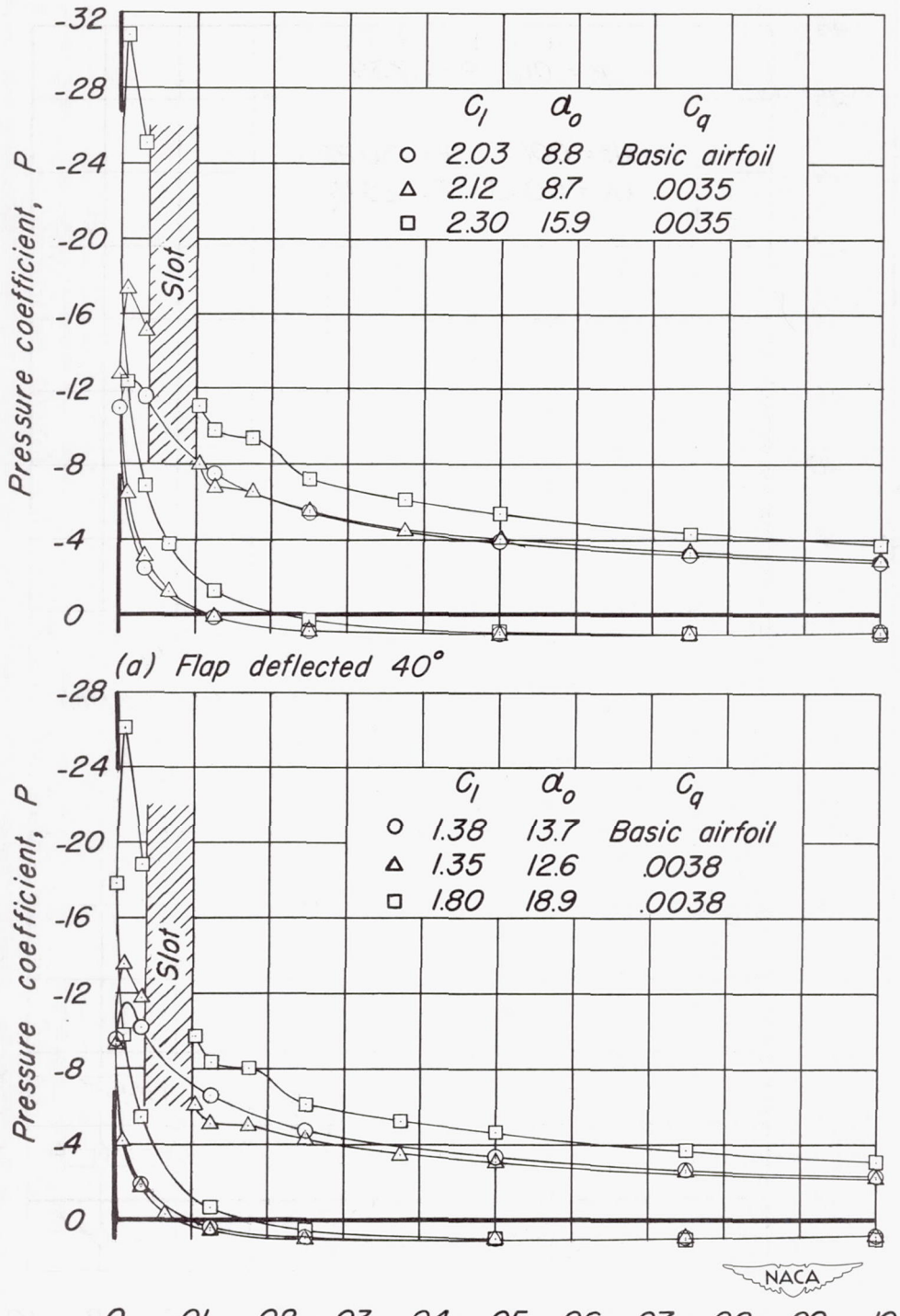

(b) Flap undeflected

Figure 10.- Detailed pressure distribution in the vicinity of the suction slot. Slot 15.

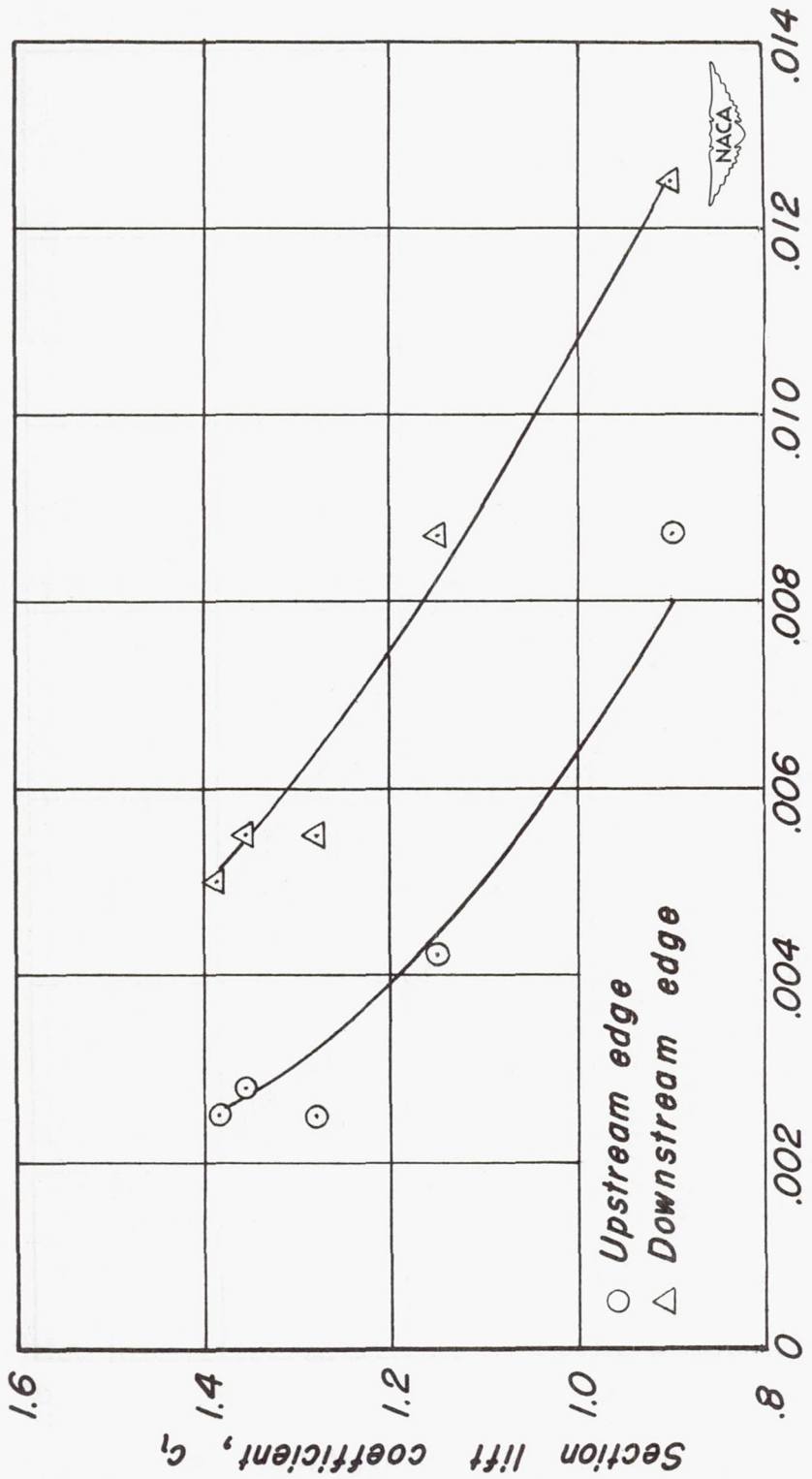

Figure 11.- Extent of the band of froth on the basic airfoil as indicated by liquid film.

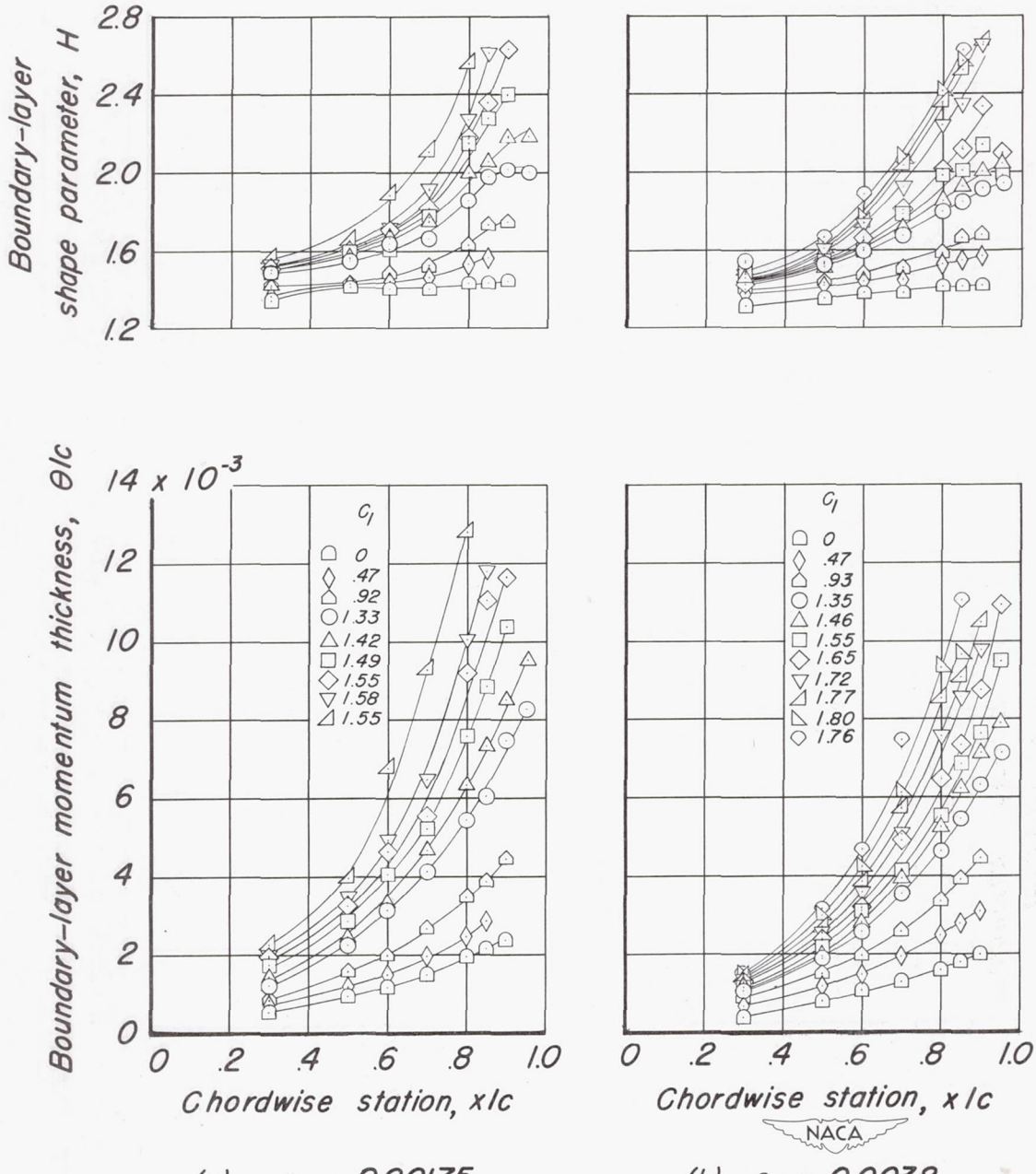

(a) c_q = 0.00175 (b) c_q = 0.0038

Figure 12.- Chordwise variation of the boundary-layer shape parameter and momentum thickness. Slot 15.

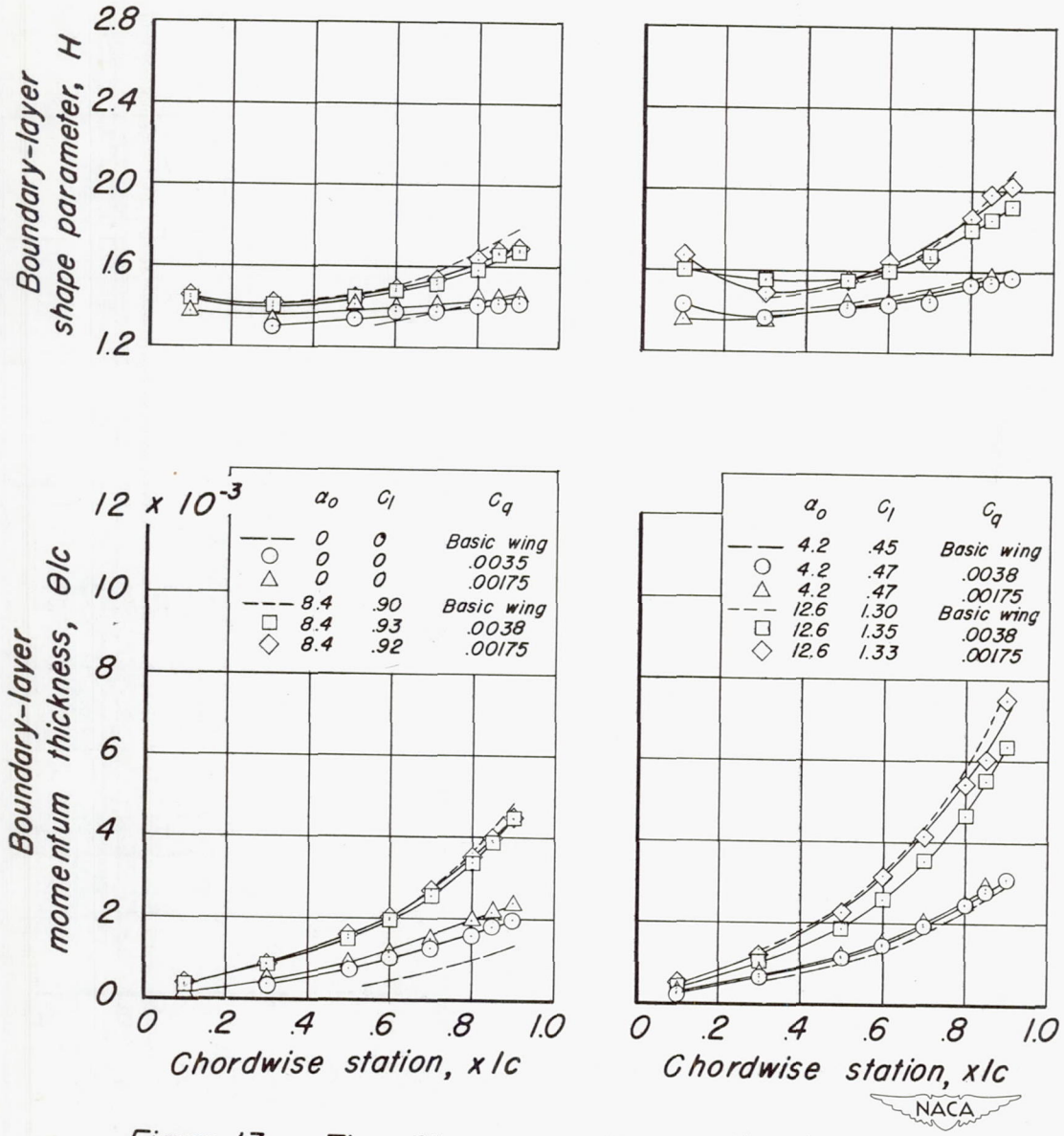

Figure 13.- The effect of suction on the boundary-layer characteristics. Slot 15.

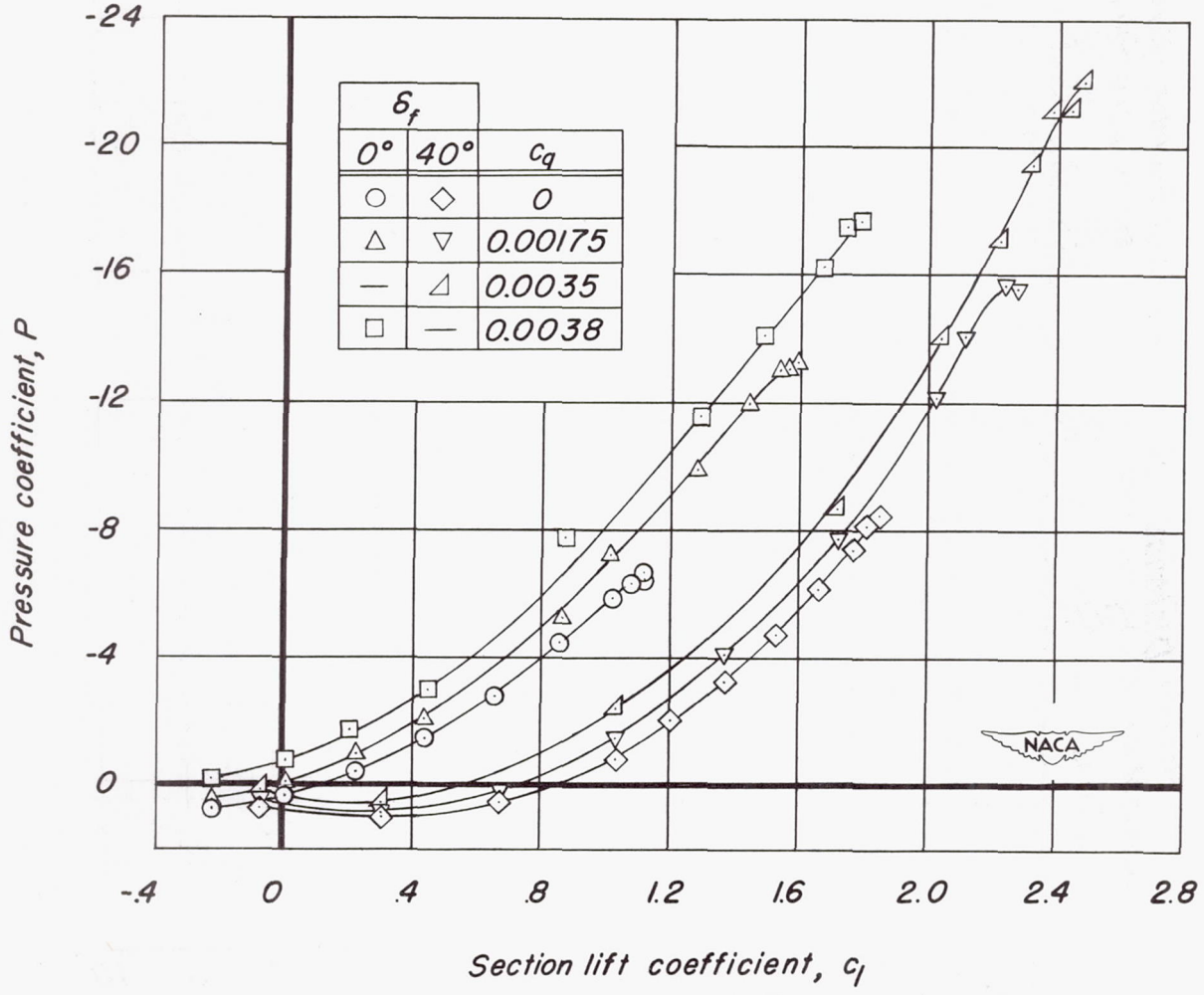

Figure 14.- Variation of the plenum-chamber pressure with lift coefficient. Slot 15.

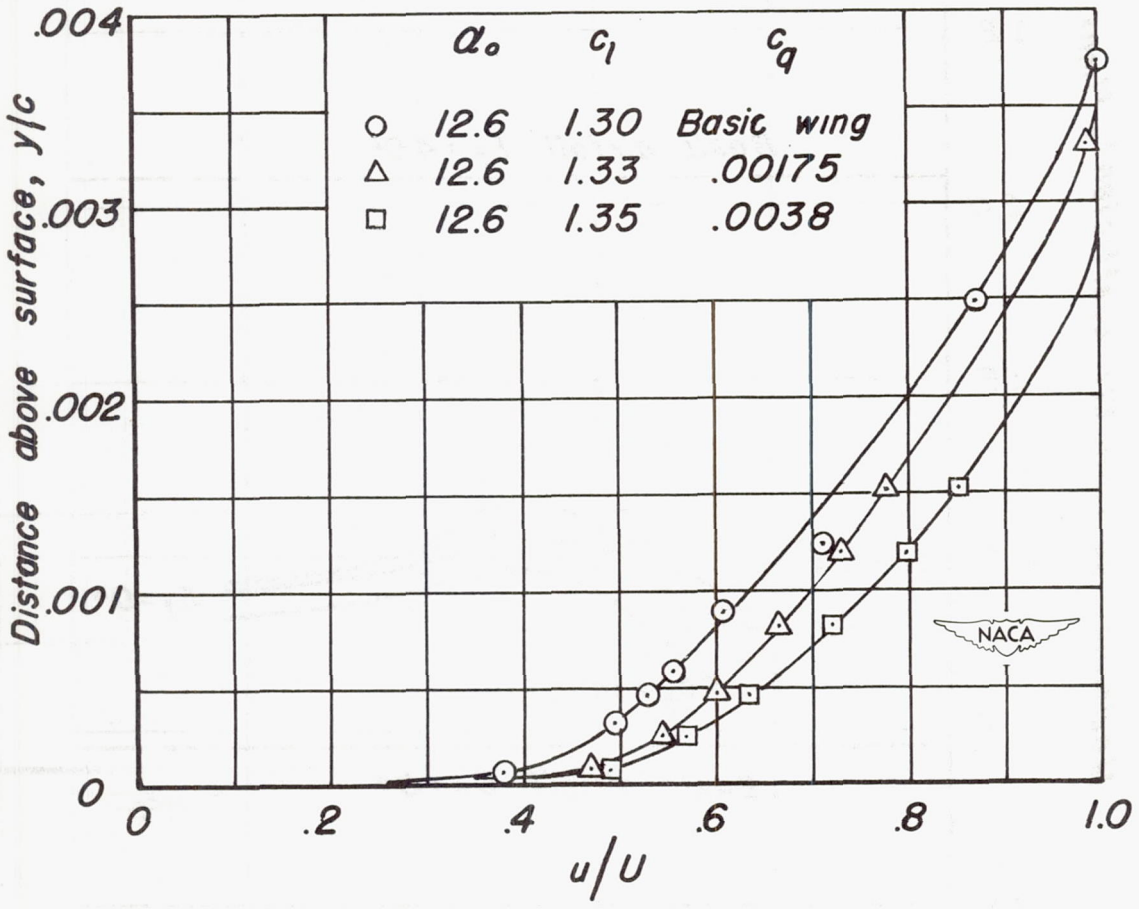

Figure 15.- Boundary-layer velocity profiles at x/c = 0.10. Slot 15.

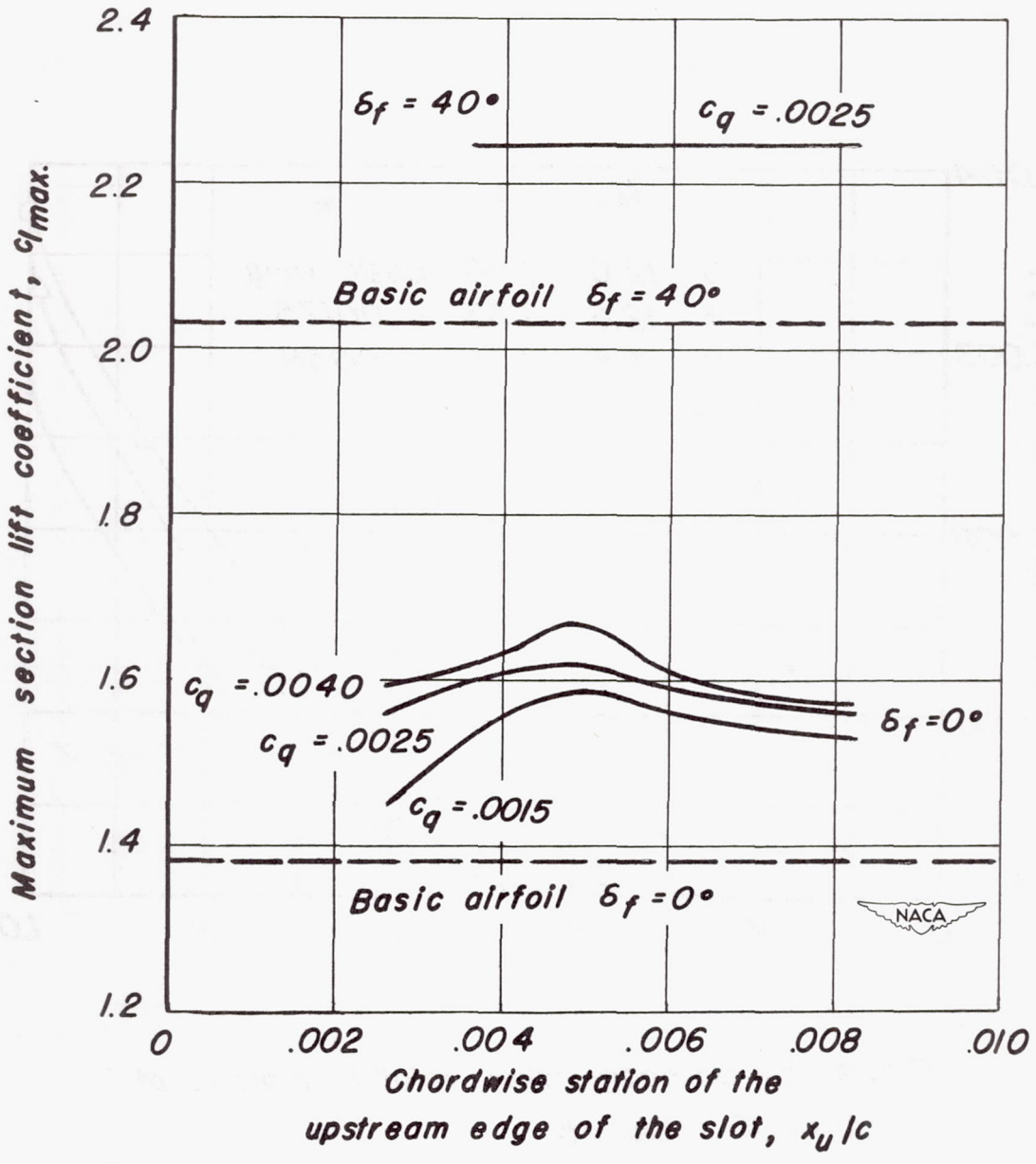

(a) $w/c = 0.002$

Figure 16.- Variation of slot effectiveness with chordwise location of the slot.

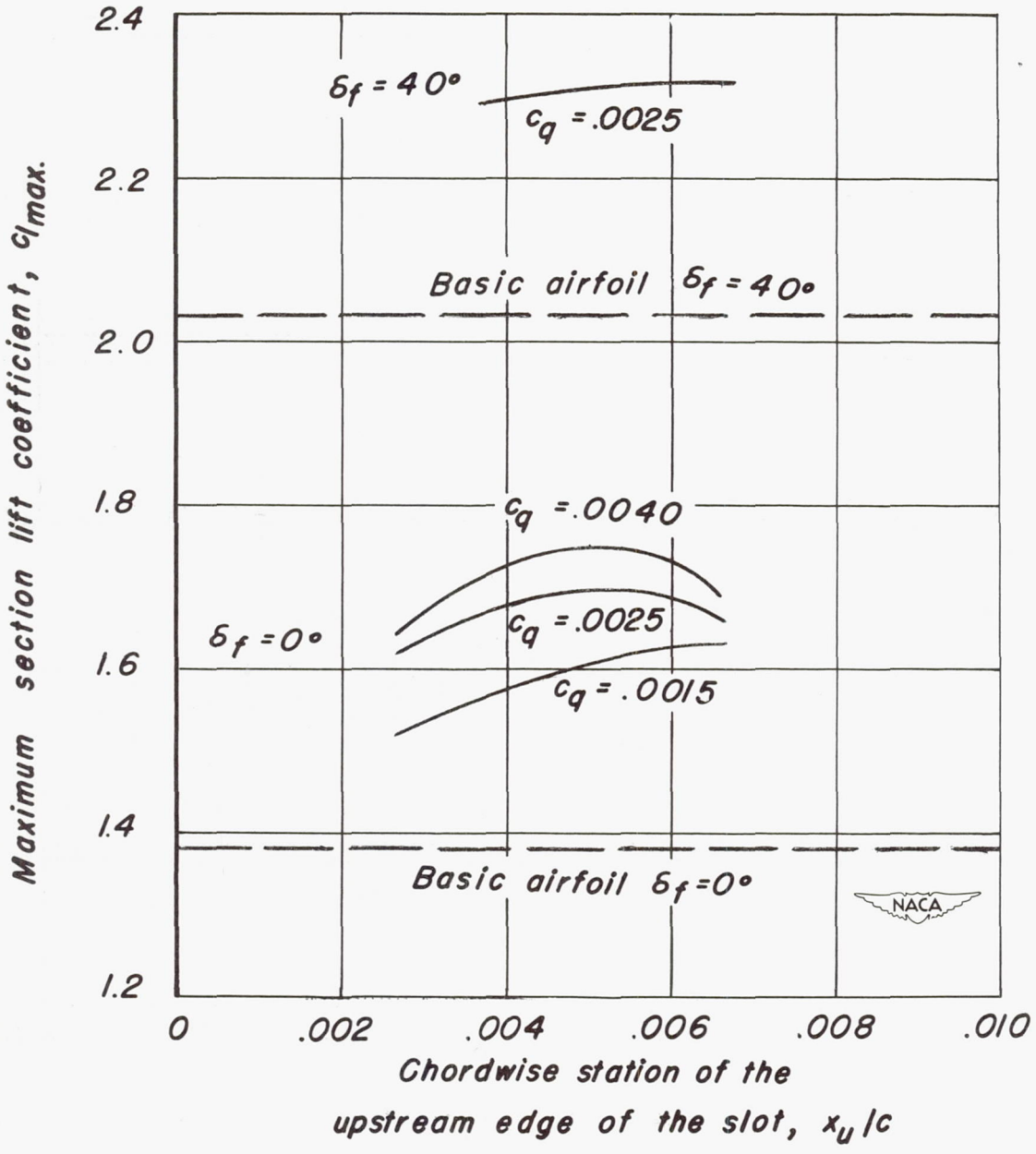

(b) $w/c = 0.004$

Figure 16.- Continued.

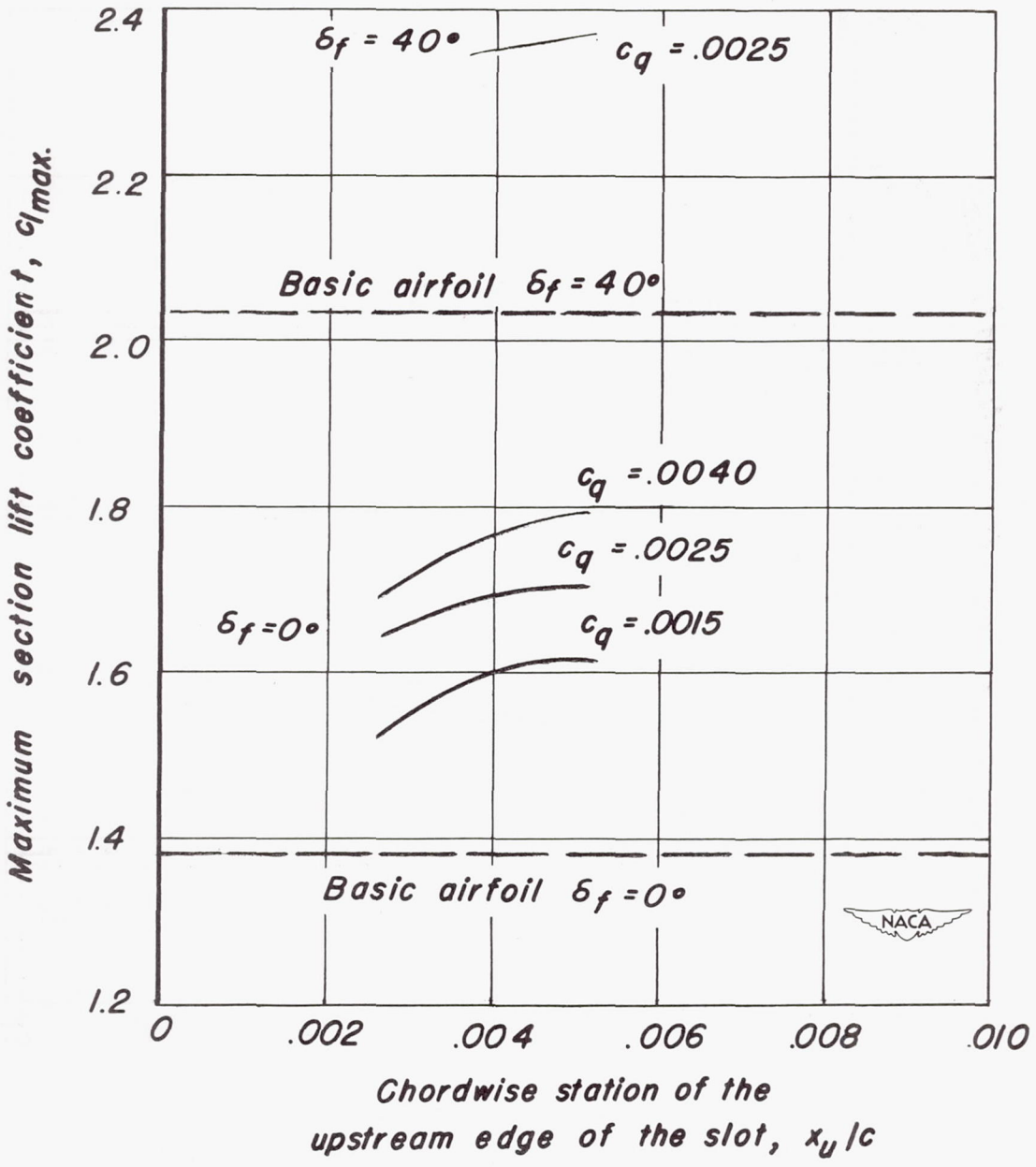

(c) $w/c = 0.006$

Figure 16.- Continued.

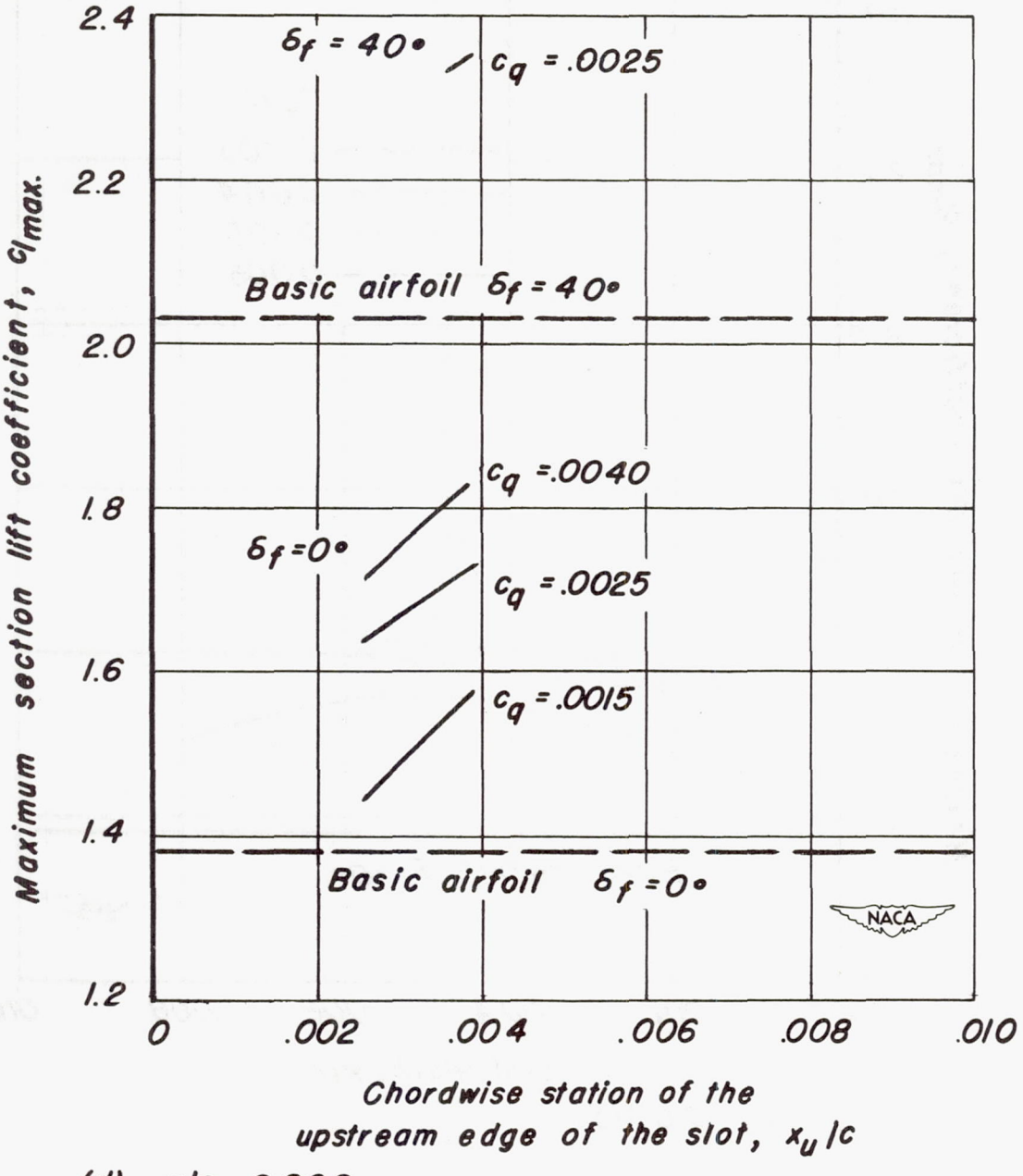

(d) $w/c = 0.008$

Figure 16.- Concluded.

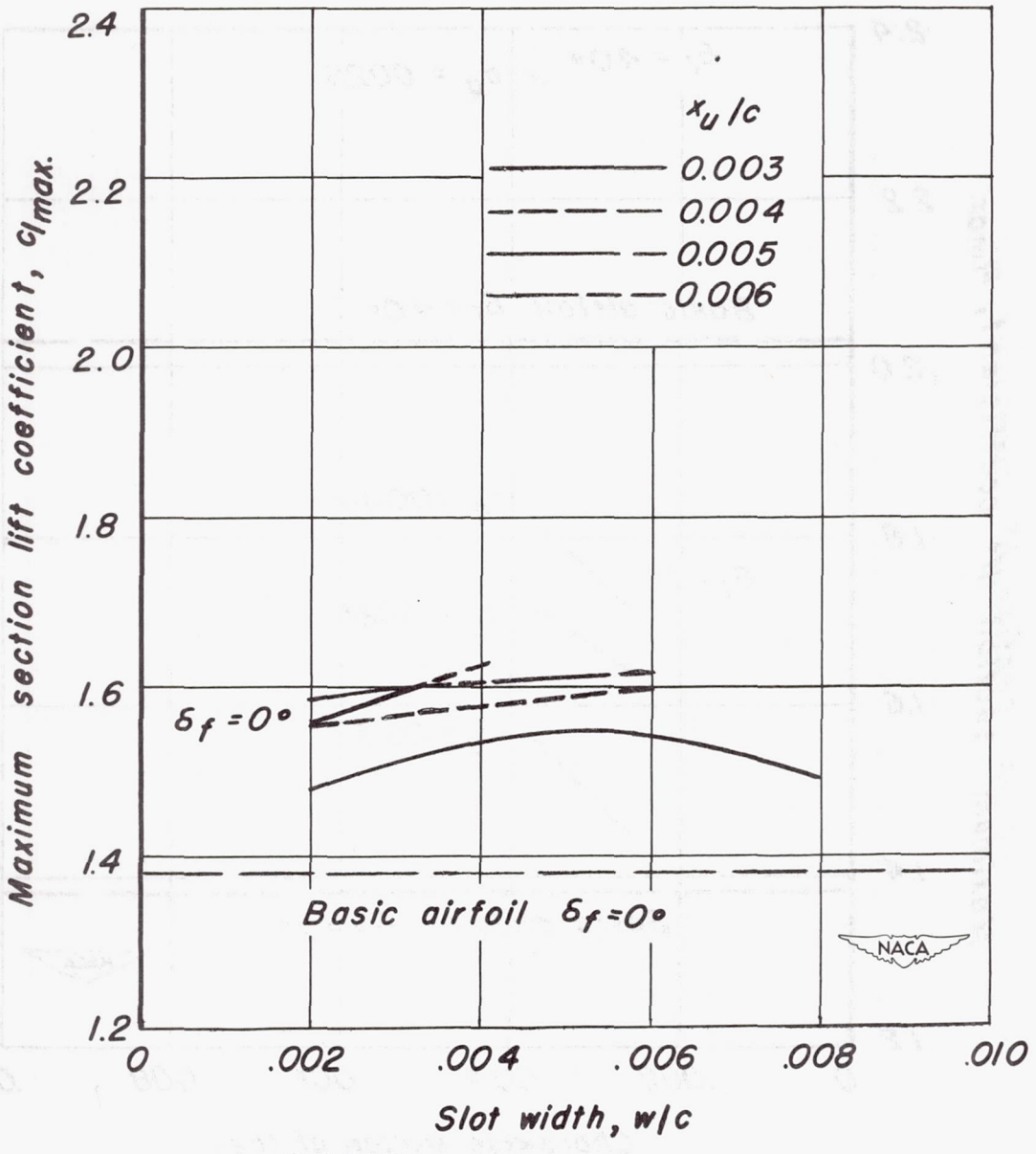

(a) $c_q = 0.0015$

Figure 17.- Variation of slot effectiveness with slot width.

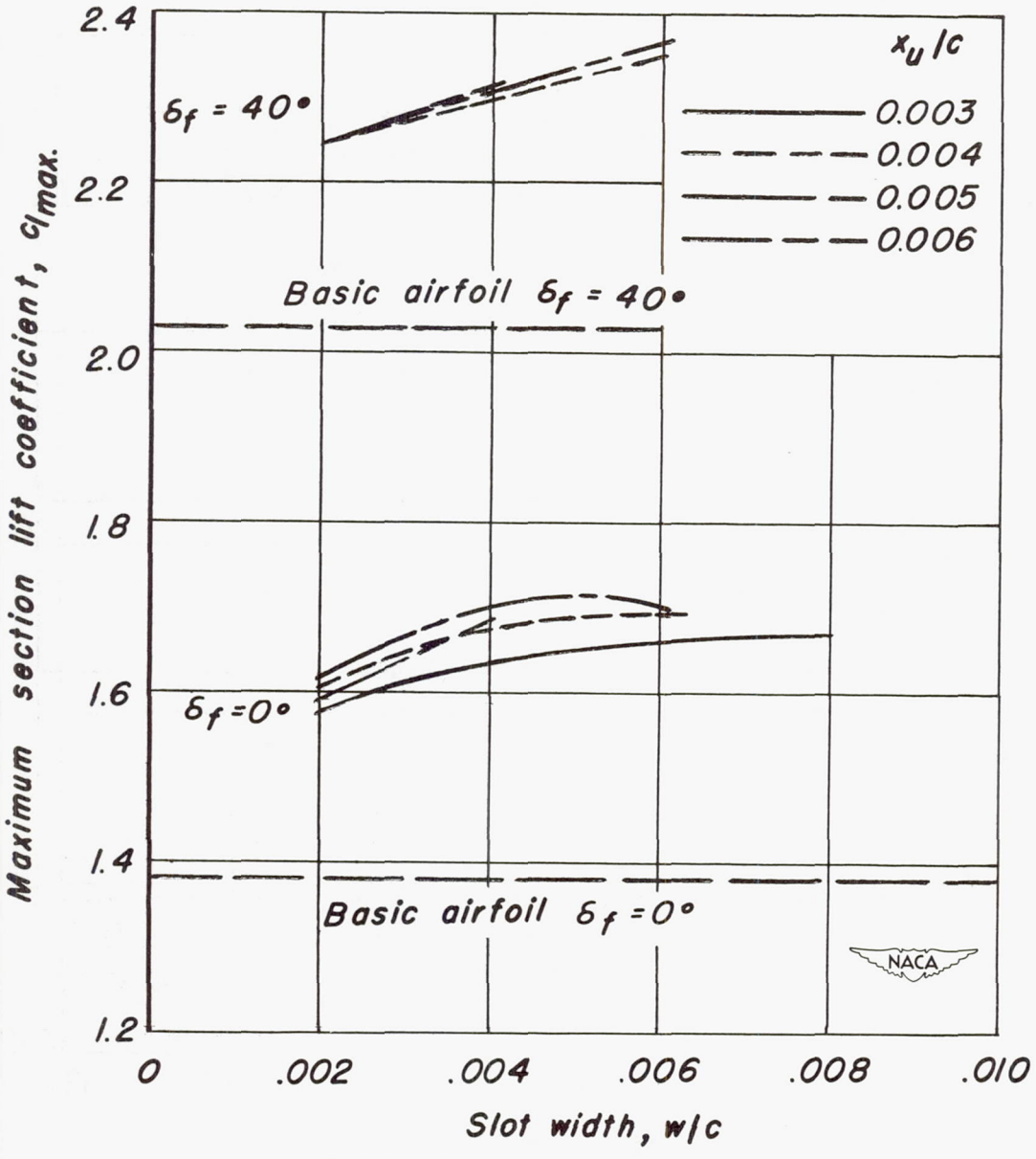

(b) $c_q = 0.0025$

Figure 17.- Continued.

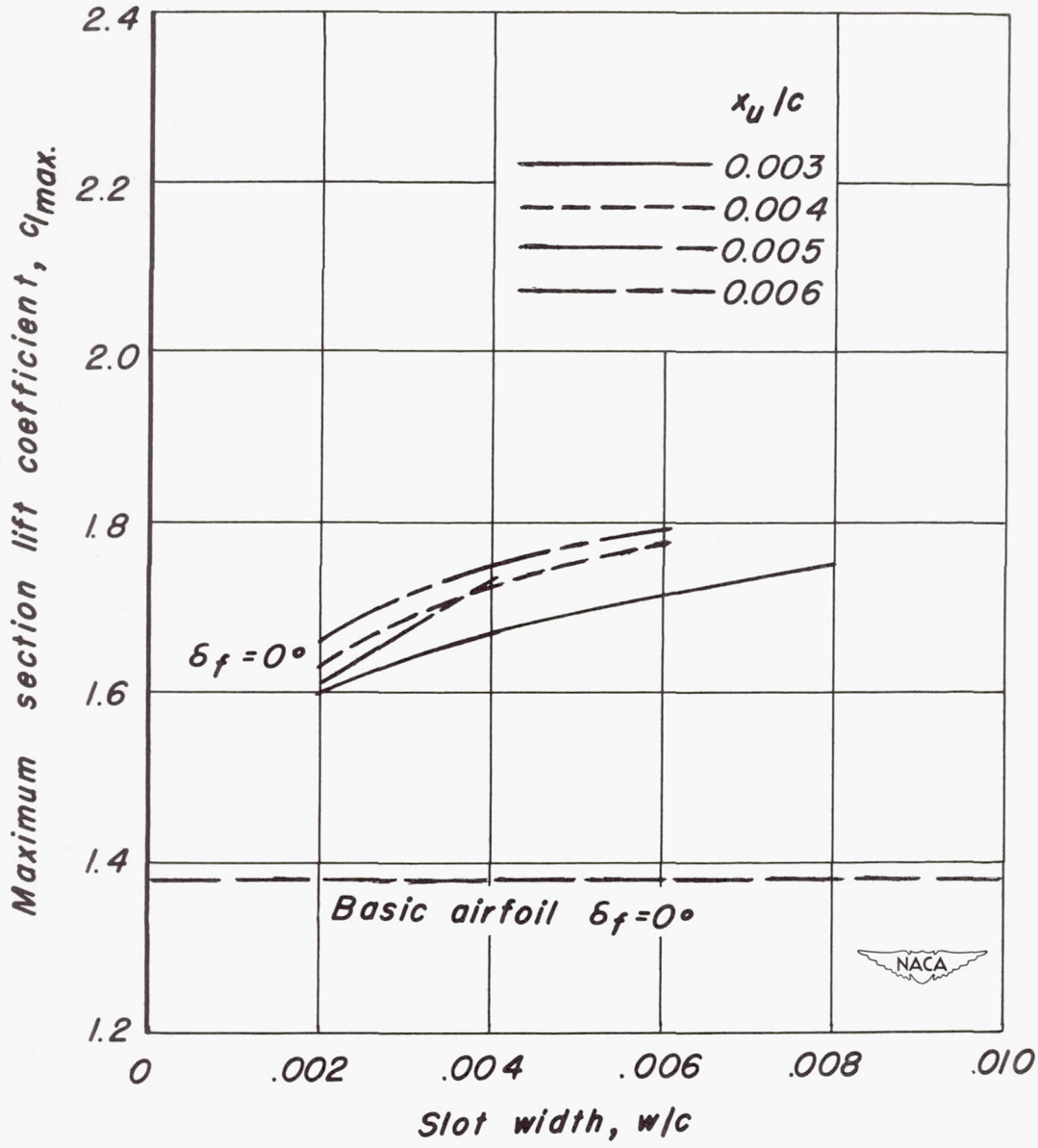

(c) $c_q = 0.0040$

Figure 17.- Concluded.